RJ 6608 (63919) 12/16/88
Magnetic Recording

IBM Confidential

Research Report

PERFORMANCE COMPARISONS OF PEAK DETECTION AND PARTIAL RESPONSE / MAXIMUM LIKELIHOOD DETECTION

Thomas D. Howell

IBM Research Division
Almaden Research Center
650 Harry Road
San Jose, California 95120-6099

Hemant K. Thapar

IBM General Products Division
Magnetic Recording Institute
5600 Cottle Road
San Jose, California 95193

IBM Research Division
San Jose . Yorktown . Zurich

Copies may be requested from:
IBM Thomas J. Watson Research Center
Distribution Services
Post Office Box 218
Yorktown Heights, New York 10598

RJ 6608 (63919) 12/16/88
Magnetic Recording

PERFORMANCE COMPARISONS OF PEAK DETECTION AND PARTIAL RESPONSE / MAXIMUM LIKELIHOOD DETECTION

Thomas D. Howell

IBM Research Division
Almaden Research Center
650 Harry Road
San Jose, California 95120-6099

Hemant K. Thapar

IBM General Products Division
Magnetic Recording Institute
5600 Cottle Road
San Jose, California 95193

ABSTRACT: This report compares the performance of Class IV Partial Response Maximum Likelihood (PRML) detectors against conventional peak detectors on two magnetic recording channels. The conventional channels are the (2,7)-coded 3380E channel with an inductive film head and the equalized (1,7)-coded channel once proposed for the Jenner product with a magnetoresistive head. Both channels use particulate disks. Results based on measured and simulated performance of the two detection methods are described. Measured off-track capability of the two systems is also compared. It is shown that PRML can provide about a 30% increase in linear density on either channel.

Introduction

Theoretical and modeling studies have shown that partial-response channels with maximum-likelihood detection (PRML) can allow magnetic recording systems to operate at higher bit densities than is possible with conventional peak detection. In order to demonstrate the benefits or PRML, the magnetic recording group in Zurich designed and built a high-speed prototype PRML channel suitable for use on high-end disk storage devices. This report describes experiments comparing that channel to the standard (2,7)-coded peak detection channel used in the 3380E disk storage unit and to the equalized (1,7)-coded peak detection channel once proposed for the Jenner product. Also included in the latter comparison is a third channel alternative known as 17ML.

Magnetic transitions written on the disk are read back as pulses of alternating polarity whose widths are determined by the geometrical and magnetic parameters of the head and disk. Peak detectors require that the transitions be spaced sufficiently far apart that the interference between adjacent pulses is small. The (2,7) run-length limited code is used in the 3380 to encode data efficiently while keeping the transitions well separated. The (1,7) code used in the Soquel product and once proposed for Jenner allows slightly more pulse crowding than the (2,7) code, but has a larger clocking window. Pulse-slimming equalization is used to reduce the interference between closely spaced readback pulses. Automatic gain control in peak detection channels is accomplished by holding the peak heights constant. A digital signal is generated which has positive-going edges marking the analog positions of the peaks in the readback signal. This signal is sent to a clocking circuit which derives both timing information and the digital data from the peak positions. Peak detection has the following advantages. It is simple and inexpensive. It allows sharing of common clocking and timing recovery circuits by several head/disk assemblies. Its performance is not impaired by channel bandwidth increases, so that when performance is satisfactory at the inner radius of the disk it is usually satisfactory at all other radii.

In partial-response channels such as PRML, transitions are placed closer together than would be allowed with peak detection. They overlap and interfere with each other. An analog-to-digital converter (ADC) samples the the readback signal. The remainder of the processing is done on the sequence of digital sample values. Partial-response class IV equalization causes the pulses to be shaped such that the samples of an isolated pulse are . . . , 0 0 0 1 1 0 0 0, ... This makes the intersymbol interference simple enough to be unscrambled by a Viterbi detector of low complexity. Timing and gain control in a PRML channel are accomplished by processing the digital sample values. The gain is adjusted to keep the absolute values of the nonzero samples near a specified value. The timing is adjusted to make the sampling errors uncorrelated with the slopes of the readback signal at the sampling times. The primary advantage of PRML is that it allows operation at a lower signal-to-noise ratio (SNR) than peak detection. This SNR advantage can be translated into increased linear or track density or improved mechanical tolerances. It uses a lower clock frequency for a given user data rate, and its digital control loops provide more frequent corrections and are less sensitive to noise and thermal drifts than are the analog loops used for peak detection.

The 17ML channel shapes the readback signal so that the isolated transition response has samples . . . , 0 0 0 .5 1 .5 0 0 0, ... It uses the (1,7) code to keep the transitions spaced at least 2 clock periods apart. Its advantages are that it provides higher storage density than peak detection and does not increase the transition density. It uses the same clock frequency as (1,7) peak detection.

Our comparison of the 3380E peak detection channel with PRML involved three kinds of tests. The first test was designed to verify that the PRML hardware was performing as designed. A channel simulation filter was used in place of the magnetic read/write channel. Noise was injected into the channel, and the error rate was

measured as a function of the injected noise level. It is easy to predict the result of such an experiment theoretically and to compare with the experimental results. Defects, mechanical problems, and magnetic nonlinearities are all factored out in this initial experiment. The second experiment replaced the simulation filter with a magnetic channel. Error rates for both peak detection and PRML channels were measured for various levels of injected noise. The results were compared with the simulation filter results and modeling predictions. Finally, the injected noise was replaced by adjacent track interference. The recording head was moved off-track into old information, and the error rate was measured as a function of off-track position. The experiment was repeated for both peak detection and PRML at the nominal recording density. It was repeated for PRML at increasing densities until the off-track performance was reduced to being comparable with peak detection. All the recording experiments were repeated at inner, middle, and outer track radii.

Our comparison of the Jenner peak detection channel with PRML involved modeling and experimental work. A third detector was included in the comparison. It was a (1,7)-coded partial-response channel with a maximum-likelihood detector known as 17ML, [1]. The modeling work was designed to determine the density gains of 17ML and PRML over peak detection under nominal conditions at a fixed error rate and to study the sensitivity of each detector to several kinds of channel impairments. Error rates for all three channels were computed using the error rate model for various recording densities. The error rates were recomputed assuming various channel impairments: extra noise, disk defects, misequalization, and timing offsets. Some experimental error rate measurements were made to check the accuracy of the model calculations. The agreement was good for the PRML detector and good to excellent for the peak detector depending on the choice of equalizer. No experimental results were available to compare with the 17ML calculations. Most of the experimental comparison of the three Jenner detection alternatives was done using slightly higher

performance particulate disks (coercivity 940 Oe) than were used for the model calculations (coercivity 840 Oe).

The experimental comparison was performed using MR heads with readback widths ranging from 5.25 to 8.75 μm. Also included in our comparison is an MR head/metal film disk combination. Old information and squeeze tests were performed at several linear densities to compare the performance of the two detection methods. The linear density was varied by changing the rotational speed of the disk and the radial position of the head. The data rates for PRML and (1,7)-coded peak detection were 3.9 MB/s and 4.3 MB/s, respectively.

In remaining sections we cover the methods used to model peak detection, 17ML, and PRML performance. We give three kinds of results for the 3380E channel: simulation filter, on-track noise injection, and off-track. We describe the modeling comparison of peak detection, 17ML, and PRML on the Jenner channel under nominal and impaired conditions, and we describe the experimental results.

Analysis Methods

One of the goals of the 3380E study was to use the model to check that the experimental hardware for both peak detection and PRML was working up to theoretical expectations. Modeling also allows us to factor out undesired differences in the experimental configurations and to explore a wider range of conditions than is possible in the laboratory.

An early version of the peak detection model is described in [2]. The peak detection model assumes linear superposition of transition responses and additive colored Gaussian noise. It uses the measured transition response to construct readback waveforms using linear superposition and the measured noise spectrum to

compute the variances and autocorrelations of the equalized noise and its derivative. The effects of precompensation and equalization are also included. The probability that a given transition is detected erroneously depends on the interference it sees from its neighbors. For each combination of neighboring bits allowed by the code, the model computes the missing-bit and peak-shift error probabilities. The overall error rate is the average of the pattern-specific error probabilities weighted by the probabilities of occurrence of the patterns.

For the 3380E experiment, the peak detection channel modeled was the product channel. The actual (2,7) code was approximated by the ideal (2,7) code, and the modified Butterworth filter was modeled by a 10-tap delay line with 12 ns spacing whose tap weights were chosen to match the response of the actual filter. Precompensation values were chosen for best performance.

Two major enhancements were made to the model between the publication of [2] and the 3380E study. One was the addition of defects. Defects were modeled by reducing the amplitudes of the readback pulses from one or more transitions. The reduction factors were represented by a distribution derived from measurements described in [3]. The second enhancement was the capability to model PRML channels. This required changes in several areas of the model. The list of data patterns had to be expanded to include patterns without transitions in the center. The PRML error events happen when noise makes correlated changes to more than one sample value. The noise autocorrelation function must therefore be computed from the measured noise spectrum. The error probability is a function of the projection of the vector of noise samples in directions corresponding to the most likely error events.

The PRML channel used the ideal (0,4) run-length limited (RLL) code to approximate the (0,4/4) code used in the hardware. The equalizer was modeled by a

10-tap delay line with 24 ns spacing whose tap weights were chosen to minimize the sum of the mean squared equalization error and the noise variance at the equalizer output, given a hypothetical white noise input. The resulting equalizer performed slightly better than an ideal minimum-bandwidth partial-response equalizer. Modeling with the actual equalizer's output pulse showed performance within a fraction of a dB of the least-squares equalizer, indicating little room for improvement in equalization.

The model was rewritten between the 3380E study and the Jenner study. Instead of approximating by the ideal (1,7) and (2,7) codes, the new model uses the exact pattern probabilities of the implemented codes. The PRML code was still approximated by a (0,4) RLL code. Equalizers are modeled more accurately in the new model, and arbitrary partial-response polynomials are allowed. This capability allows the model to switch between PRML and 17ML by changing input parameters. No change to the program is required. The method of defect modeling was improved. Defects in the new model are represented by a reduction in magnetization by a specified factor for a specified length. The new model includes a computation of extra-bit errors, and the improved defect model is needed for this computation.

The peak detection channel for Jenner used the (1,7) code. Its equalizer had adjustable first and second derivative parameters and two identical three-pole Bessel low-pass sections with adjustable cut-off frequency. The three filter parameters and two precompensation parameters were adjusted for best performance. The PRML and 17ML equalizers used 9-tap delay lines with tap spacing equal to the clock period. The algorithm for computing tap weights was the same as was used for the 3380E study except that the actual noise spectrum was used instead of hypothetical white noise.

All the modeling work for the 3380E study was done for the recording conditions at the inner radius. The head/disk velocity is 39.84 m/s which corresponds to a

recording density of about 15.3 kbpi at 3 MB/s. The unequalized and equalized 3380E isolated transition responses for the peak detection channel are shown in Figure 1. The corresponding signals for the PRML channel are shown in Figure 2. The unequalized and equalized noise spectra for the 3380E peak detection and PRML channels are shown in Figure 3 and Figure 4. Figure 5 shows a measured defect size distribution for the 3380E from which the modeled defect distribution was derived.

The model was used to predict the error rates of peak detection, PRML, and idealized PRML for the 3380E in the presence of varying amounts of injected white noise. The idealized PRML detector assumes perfect equalization to class IV partial-response sample values, while the PRML detector uses the tapped delay line previously described. The results were compared with the experimental measurements of error rates with peak detection, PRML on the equalized magnetic channel, and PRML on the channel simulation filter. The results are shown in Figure 6. There is excellent agreement between the model and experiment for peak detection and between idealized PRML and the measurements on the channel simulation filter. The experimental results for PRML on the magnetic channel differ from the model results by about 2 dB. The model says the PRML channel tolerates about 7 dB more injected noise at the inner radius than the peak detection channel at 10^{-8} errors/bit. The measurements indicate only a 5 dB difference. The data rate for PRML was then increased until the error rate performance was comparable to that of the 3 MB/s peak detector. Comparable performance was reached at 4 MB/s for PRML, and this curve is included in Figure 6. This is a 33% higher density than (2,7)-coded peak detection. This increase is in excellent agreement with the experimental value of 30% which will be described later.

The PRML curves on Figure 6 tend to flatten at low levels of injected noise. The reason is that defects begin to dominate the error rate. The performance of PRML in

the presence of defects can be improved by biasing the gain, i.e., setting the gain slightly higher than the nominal value so that gain reductions due to defects are less damaging. This is analogous to lowering the clip level in a peak detector. The defect sensitivity of PRML without gain bias is similar to that of a peak detector with a clip level of 50%. The peak detector model uses a clip level of 40%, so it is somewhat less sensitive to defects.

The Jenner modeling assumed a head/disk velocity of 21.92 m/s corresponding to about 40 kbpi at 4.3 MB/s. The velocity was held constant, and density was adjusted by changing data rate. The unequalized and equalized Jenner isolated transition responses for the peak detection channel are shown in Figure 7. The corresponding signals for the 17ML and PRML channels are shown in Figure 8 and Figure 9. The unequalized and equalized noise spectra for the Jenner peak detection, 17ML, and PRML channels are shown in Figure 10, Figure 11, and Figure 12.

The model was used to predict the error rates of peak detection, 17ML, and PRML for Jenner under nominal conditions. The densities were 35, 40, and 45 kbpi for peak detection, 40, 45, and 50 kbpi for 17ML, and 45, 50, and 55 kbpi for PRML. The densities were chosen to produce error rates from well below 10^{-9} to well above it under nominal conditions. The results were compared with the experimental measurements of error rates with peak detection at 45 and 50 kbpi and PRML at 50 and 55 kbpi. The error rates predicted for lower densities are too low to measure. No data were available for these components with 17ML. The nominal condition error rates are shown in Figure 13 along with the experimental points. An additional peak detection curve shows the modeled performance with filter parameters which represent a less aggressive approach to equalization. The measured points for peak detection fall between this curve and the one representing the optimal equalizer, but are much closer to the curve for the suboptimal equalizer. This suggests that the equalizer used with

the peak detection hardware is better represented by the suboptimal equalizer in the model. The experimental points for PRML are not far from the model predictions, but the dependence on density is much less than expected. One possible explanation is that the error rates are dominated by disk defects. The density at which each detector's error rate reached 10^{-9} was computed. The 17ML and PRML detectors achieved densities 23% and 34% higher than peak detection with the suboptimal equalizer, respectively. The corresponding gains over peak detection with the optimal equalizer were 23% and 11%.

One of the objectives of the Jenner study was to determine the sensitivity of the three detectors to various kinds of channel impairments. To simulate the effect of increased electronics noise which might be expected at high data rates, the portion of the noise from the electronics was doubled while keeping the signal and disk noise fixed. The performance of all three detectors degraded about equally. The results are shown in Figure 14. The results for nominal conditions are included for comparison. To compare the sensitivities of the detectors to defects, we modeled their error rates at the site of a 75% defect one user bit (about .5 μm) long. The results are shown in Figure 15. The effects on the peak detector and PRML were similar, while the effect on the 17ML detector was larger. The effect of misequalization was modeled by changing the width of the isolated transition response by $\pm$ 7.5% with equalization and other factors held constant. The wider pulse hurt the performance of all three detectors with peak detection being hurt the least. The narrower pulse improved the performance of peak detection at all densities and PRML at its highest density because it reduced the interference between pulses. It hurt the performance of 17ML and of PRML at the lower densities because it made the equalization incorrect. These results are shown in Figure 16. The effect of timing jitter was modeled by offsetting the clock by $\pm$ 1 and $\pm$ 2 ns relative to the readback signal. For each detector, the effect of positive and negative offsets was very similar, and the effect of a 2 ns offset was

somewhat more than twice the effect of a 1 ns offset. Peak detection was least sensitive to timing offsets. The 17ML detector was slightly more sensitive than PRML. The results are shown in Figure 17.

Performance Measurements

This section compares the real-time performance of PRML to (2,7)-coded peak detection on the 3380E head/disk components, and to (1,7)-coded peak detection on magnetoresistive (MR) head/particulate disk and MR head/metal film disk components. We first give an overview of the signal processing functions in each detector and the experimental set-up used. The remaining section describes the measured performance of the different detectors.

PRML versus (2,7)-Coded Peak Detection for 3380E

The hardware for the PRML detector was designed and built by the Magnetic Recording group, IBM Research Laboratory, Zurich, using off-the-shelf analog and digital circuits. The prototype channel, referred to here as "ZPRML prototype", uses seven cards which implement the various read, write, and detection functions shown schematically in Figure 18. For more details of the hardware, refer to [4].

Customer data in NRZ format is input to the write control card, where it is encoded using the (0,4/4) run-length code [5]. The write control also generates prescribed training patterns to synchronize the timing and the gain control loops. The encoded data waveform can be applied to a magnetic recording channel, or an electronic filter that simulates the Class IV partial-response spectral characteristics (also referred to as "channel simulation filter" in this report). The latter option is useful for isolating malfunctions in the prototype hardware. The output of the channel simulation filter is a 3-level signal which can be applied to the ZPRML prototype to evaluate the performance of PRML. Figure 19 (a) shows such a signal in the form of

the so-called "eye diagram," which is obtained when the analog data signal to the oscilloscope is suitably triggered with the readback clock signal.

When the magnetic recording channel is interfaced to the ZPRML prototype, the readback signal is first equalized with a linear RLC or a tapped delay line filter. The output of a properly designed equalizer is a 3-level signal, similar to the output of the channel simulation filter. Figure 19(b) shows such a signal derived by equalizing the readback signal from the 3380E head/disk components. The fuzziness in the waveform of Figure 19(b) is due to higher system noise. The equalizer response is determined analytically based on the recording channel response and the desired Class IV response. The recording channel response is itself derived analytically using the least-squares identification method [6]. The identified response is used in a computer program to perform pole/zero placement and determine the required element values of the RLC filter. A sixth-order filter, comprising 3 second-order RLC filter sections, was typically required to perform the equalization. The RLC filter was subsequently replaced by an analog tapped delay line filter, whose tap weights were determined analytically by minimizing the mean squared-error between the identified channel response and the desired Class IV response. The tapped delay line filter functioned as a compromise equalizer for a given head/disk combination. Further equalization to compensate channel response variations from the outer diameter (OD) to the inner diameter (ID) was provided by a digital cosine equalizer [7] whose tap weight was determined adaptively in the hardware.

The output of the equalizer or the channel simulation filter is applied to the analog card which contains the analog portions of timing and gain control loops and the analog-to-digital converter (ADC). On the analog card, the input signal is first level-adjusted with an automatic gain control (AGC) amplifier. The AGC output is sampled with a 6-bit linear ADC whose clock is also generated on the analog card.

The samples from the ADC are distributed to the Viterbi detector, the digital adaptive cosine equalizer, and the digital timing and gain control cards. The Viterbi detector performs maximum-likelihood sequence estimation based on minimization of the squared-error between the input and the ideal (noise-free) sample sequences. The output of the Viterbi detector is applied to the read control card which decodes the received (0,4/4) data. The decoded data is compared to the customer data to obtain the error statistics. A prescribed set of intermediate (tentative) decisions in the Viterbi detector is also applied to the digital timing and gain control cards to update the nominal values of the gain and the clock frequency. The control of the timing and gain loops is based on the well-known stochastic gradient algorithm [8].

The performance of (2,7)-coded peak detection was measured with the 3380E read/write channel, called "Polecat channel" in San Jose. The channel hardware, whose schematic diagram is shown in Figure 20, was optimized for 3380E head/disk combination, (2,7) run-length limited code, and 3 MB/s customer data rate. Customer data is encoded using a (2,7) code, and recorded in NRZI format. The presence of a transition at the clock instant represents a "1", and its absence represents a "0". The readback signal is amplified, level-adjusted by an AGC amplifier, and then applied to a modified third-order Butterworth low-pass filter with nominal 3-dB bandwidth of 16 MHz to limit the noise power. The filtered AGC output is clipped, full-wave rectified, and differentiated. The level of the rectified signal and the zero crossings of the differentiated signal are used to locate the presence or absence of transitions, or equivalently 1's and 0's.

The performance of (1,7)-coded peak detection method was measured with hardware once proposed for the Jenner product. The channel was optimized for MR head/particulate disk, (1,7) run-length code, 4.3 MB/s data rate, and 50 kbpi linear density. This channel used a higher-performance disk than was used to generate the

input data for the modeling work. The densities achieved with this disk are not directly comparable with the modeling results. The signal flow in this channel was similar to that for the (2,7)-coded peak detector. The specific design parameters, however, were different because of different operating points of the two channels. A major difference in signal processing in the (1,7)-coded peak detector was the use of pulse slimming equalization instead of the modified Butterworth low-pass filter.

The experimental setup used for the performance comparison of the detection methods is shown in Figure 21. A computer-controlled tester was used to perform the read/write and error checking functions. When evaluating PRML, the tester was configured to allow (0,4/4)-encoded data sequences to be applied either to a magnetic recording channel or a channel simulation filter . The capability to switch channels was intended to facilitate debugging and isolating hardware problems in the experimental set-up. Indeed, the channel simulation filter was used periodically to ensure proper functioning of the ZPRML prototype and adjust for any drifts in parameters due to aging, etc. In the case of peak detection, the tester was configured to allow either (2,7)- or (1,7)-coded sequences to be recorded. The performance comparison of the two methods in the sequel is based on readback signals that were derived using the same arm electronics (AE) modules.

The performance of the ZPRML prototype was first characterized at a data rate of 3 MB/s with a channel simulation filter. Bit error rate was measured as a function of signal-to-noise ratio (SNR) with active and inactive timing and gain control loops, and compared to that of ideal PRML system. As shown in Figure 22, the measured performance agrees within 0.2 dB of the theoretical performance of PRML on additive white Gaussian noise channel, thereby indicating negligible performance loss in implementation. Even with active loops, the performance loss is about 0.5 dB relative to the ideal system. These performance tests show that the adaptive timing and gain

loops are well-designed, the 6-bit quantization of the readback signal is adequate,[1] and the hardware works well.

Tests were also performed to examine the transient behavior of the control loops. Figure 23 shows the transient behavior of the timing and gain loops under various conditions of noise, gain offset, and frequency offset. The convergence shown in the figure agrees well with simulation results [9]. All tests related to transient behavior showed that the loops converged reliably to nominal values, yielding expected steady-state performance.

The performance comparison of PRML and (2,7)-coded peak detection methods was performed on 3380E inductive film head and particulate disk components. The nominal 3380E operating point is defined by 3 MB/s, 16.2 kbpi at the inner radius of 99 mm, and 1386 tpi. Our modeling and experimental work was done at the slightly larger inner radius of 105 mm corresponding to 15.3 kbpi.

Two types of tests were performed to compare the performance of the detection methods. First, ontrack error rate was measured in the presence of different levels of noise, injected at the input of the preamplifier. Second, offtrack capability was measured for the two detection systems in the presence of different old information. The noise injection tests were also used to i) ascertain the performance loss for PRML on a magnetic recording channel relative to an ideal additive white Gaussian noise channel, and ii) verify the approximate 3dB gain in SNR due to maximum likelihood sequence estimation.

---

[1] More than 6 bits may be required when significant equalization is performed after the ADC.

Figure 24, Figure 25, and Figure 26 show for the two detection systems at 3.0MB/s customer data rate the byte error rate as a function of injected noise level at the OD, MD, and ID, respectively. The PRML performance curves are based on RLC equalizers designed individually for each radius. The curves were unchanged when the RLC filters were replaced by the analog tapped delay line and the adaptive cosine filters. The performance of peak detection was measured by applying write precompensation only at the ID.

The performance data in Figure 24, Figure 25, and Figure 26 show that, at a byte error rate of 10^{-7}, PRML can withstand 2.8dB more noise than peak detection at the OD, 3.2 dB at the MD, and 5dB at the ID. Thus, at the same customer rate, PRML provides more immunity to additive noise; that is, it yields the same error rate at a lower signal-to-noise ratio than peak detection. How one uses the extra noise immunity depends on the application. One can, for example, increase the overall areal density by increasing the track density or linear density, or both. The advantage may be also used to relax flying height requirements or achieve higher yields in HDA manufacturing at a given level of component tolerances.

We chose to use the extra noise immunity to increase the linear density to the point where the performance of PRML was comparable to that of peak detection at 3.0 MB/s. Figure 27 shows the byte error rate as a function of injected noise at the ID, with peak detection operating at 3 MB/s, and PRML at 3.6 and 3.9 MB/s. At 3.6 MB/s (20% higher density), the PRML performance is still better than that of peak detection; at 3.9 MB/s (30% higher density), the performance of the two systems is comparable. The relative increase in linear density agrees well with the modeling results given in Figure 6.

The performance of PRML on additive white Gaussian noise channel is easy to understand and analyze. Indeed, the probability of error under ideal conditions is given by

$$P_e = Q(\sqrt{SNR})$$

where SNR is the ratio of the signal power to noise power, and Q(x) represents the area under the tail of the Gaussian density function, and is given by

$$Q(x) = \frac{1}{\sqrt{2\pi}} \int_x^{\infty} e^{-\frac{t^2}{2}} dt$$

To assess the performance loss for PRML on a magnetic recording channel relative to the ideal white Gaussian noise channel, the byte error rate as a function of rms-signal-to-rms-noise ratio was measured. Figure 28 shows the performance of PRML on the 3380E components and on the ideal white Gaussian noise channel. As shown, PRML requires about 1.5-2.2 db more SNR on the magnetic recording channel at a byte error rate of 10^{-7}. This difference may vary with other recording components, depending on the noise spectrum and the level of nonlinear or other uncompensated channel distortions.

Analysis of Class IV signalling on additive white Gaussian noise channel shows that maximum likelihood detection should require 3 dB less SNR than threshold detection for a given error rate. This result was verified experimentally by measuring the error rate of the first tentative decision and the final decision in the Viterbi detector. Figure 29 shows a plot of the byte error rate as function of SNR for the two types of decisions. Note that maximum likelihood detection does indeed require about

3dB less SNR than threshold detection. However, it is important to note that this advantage was measured ontrack when the injected white Gaussian noise dominated the background electronics and media noise. The 3 dB advantage of maximum likelihood detection decreases when the noise is correlated like the signal, as is the case with offtrack noise.

The performance of PRML and peak detection was also compared on the basis of their offtrack capability. Figure 30 shows the byte error rate versus offtrack position for the two systems at 3.0 MB/s. The interference bands in each case were chosen to be suitably encoded random data patterns. As shown, PRML provides approximately 20% more offtrack capability at the ID at a byte error rate of 10^{-7}. Figure 31 shows a similar plot, but with the PRML density increased by 30%. The performance of the two systems is now comparable.

The offtrack performance of PRML is degraded when the interference tracks contain only the pattern used to synchronize the timing and gain control loops, namely, the pattern which generates a sinusoid at one-fourth the bit rate. Figure 31 also shows the offtrack performance of PRML with the different interference patterns. Note that the error rate is 8-10 times higher for the case when the adjacent track contains *exclusively* the synchronization pattern. Such degradation in performance can be reduced in a product by encoding the customer data to avoid recording long run-lengths of the synchronization pattern. Indeed, the (0,4/4) code has been designed to achieve that objective. The offtrack performance of (2,7)-coded peak detector was found to be insensitive to the characteristics of adjacent track interference.

PRML versus (1,7)-Coded Peak Detection for MR Head

The performance comparison of PRML and (1,7)-coded peak detection was performed with MR heads and particulate or metal film disks. The measurements were performed on the Cambrian precision test stand with the PRML detector operating at 3.9 MB/s, and the peak detector at 4.3 MB/s. The recording density was varied by changing the rotational speed of the disk and the radial position of the head. Equalization for PRML was provided by a compromise filter, implemented on an analog tapped delay line, and the adaptive cosine filter.

Old information and squeeze tests were performed to compare the performance of the two detection schemes. The tests were used to derive the so-called alpha parameter, a commonly used performance measure for detection methods in San Jose. Alpha is defined as the ratio of the old information number to the sum of the track-pitch-to-failure and the old information number. The old information number is the off-track distance into old information at which a prescribed error criterion is reached. The track pitch to failure is the spacing at which an encroaching "squeeze" track causes a similar error criterion to be reached. An alpha of .16 (16%) or more has generally been deemed acceptable in past products.

Figure 32 shows alpha as a function of linear density for the two detection methods on a 940 Oe particulate disk and varying width of the MR head read element. At alpha of 18%, PRML provides 16 to 32 percent higher linear density than (1,7)-coded peak detection. This advantage increases with decreasing read element width. The behavior is consistent with theory and simulated results and may be understood in terms of the extra noise immunity provided by the PRML method. As the readback head width decreases, the signal-to-noise ratio also decreases. This causes peak detection to degrade faster than PRML in the operating region of interest, thereby increasing the advantage of PRML with narrower heads.

Figure 33 shows old information capability as a function of linear density for the two detection methods on a 940 Oe particulate disk and varying width of the MR head read element. At 50 kbpi, where the peak detection hardware was optimized, PRML provides approximately 18 percent more old information capability. This result is consistent with the 20 percent advantage at 3 MB/s for PRML relative to (2,7)-coded peak detection. Thus, at a given linear density, the old information advantage of PRML may be used to relax the track misregistration (TMR) requirements of the servo system.

The performance of PRML and (1,7)-coded peak detection was also compared on a 840 Oe particulate disk with MR head. The relative advantages of PRML were similar to those noted above for the 940 Oe disk. However, both systems achieved lower recording density at an alpha of 18%.

We also compared the performance of PRML and (1,7)-coded peak detection on a metal film disk to measure the effect of noise due to higher flux-change density inherent in PRML recording. Figure 34 and Figure 35 show the performance of the two detection methods on a 1300 Oe metal film disk. As shown, PRML provides about 38 percent higher linear density than peak detection at alpha of .18 and about 25% more old information capability at 60 kbpi. Even though these figures represent limited data, it does indicate that PRML can provide a significant increase in density on a suitably designed metal film disk.

Conclusions

Both modeling and experiment show the PRML channel to be superior to the (2,7)-coded peak detection channel used in the IBM 3380E. The performance difference can be quantified in several ways. The PRML channel can withstand about 5 dB more noise at the same density and error rate, it can achieve comparable

performance at 30% higher density, or it can operate 20% farther off-track at the same density and error rate as the conventional channel. The agreement between modeling and experiment is good.

Both modeling and experiment show both 17ML and PRML channels to be superior to the (1,7)-coded peak detection channel once proposed for Jenner. The linear density gains are 11-23% for 17ML and 23-34% for PRML depending on the degree of equalization used with the (1,7)-coded peak detection channel. Measurements with the hardware suggest that the true gains are near the high ends of these ranges. While both improved channels are somewhat more sensitive to channel impairments than the peak detector, modeling indicates the differences are not large.

Acknowledgements

We thank W. Hirt and W. Schott for their help on inquiries related to the ZPRML prototype and M. Condron and D. Chan for their help in the experimental work.

REFERENCES

1. A. Patel, A new algorithm for processing sample values in (1,7) coded partial response channel, Memo to File, June 23, 1987.

2. P. Siegel, Applications of a peak detection channel model, *IEEE Trans. Mag.*, **MAG-18**, No. 6, 1250-1252, Nov. 1982.

3. T. Howell, et. al., A study of disk noise statistics, *IEEE Trans. Mag.*, **MAG-22**, No. 5, 901-903, Sept. 1986.

4. F. Dolivo, R. Hermann, W. Hirt, S. Oelcer, W. Schott, and A. Vogt, The Zurich High-Speed PRML Prototype, Internal Report, April 1, 1985.

5. B. Marcus and P. Siegel, Constrained codes for PRML, RJ-4371, July 31, 1984.

6. J. Cioffi, Least-Squares Channel Identification, *IBM J. Res. Dev.*,**30**, pp. 310-320, May 1986.

7. F. Dolivo, R. Hermann, W. Hirt, S. Oelcer, A. Ruengeler, W. Schott, and A. Vogt, Digital Implementation of an Adaptive Cosine-Equalizer for the Zurich High-Speed PRML Prototype, Internal Memo, Feb. 14, 1986.

8. S. U. H. Qureshi, Timing Recovery for Equalized Partial-Response Systems, *IEEE Trans. Comm.*, **COM-24**, pp. 1326-1331, December 1976.

9. W. Schott, Unpublished Work.

FIGURES

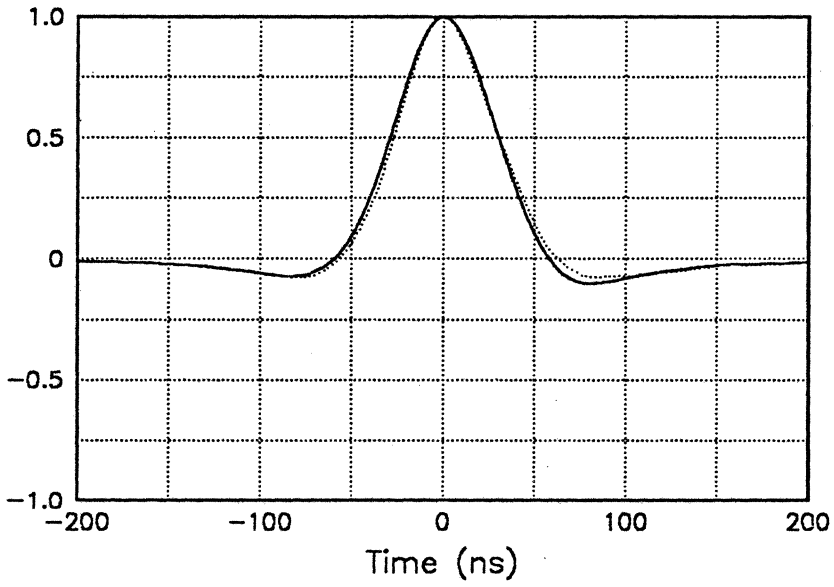

Figure 1. Isolated transition before (dotted) and after equalization for peak detection at 3.0 MB/s.

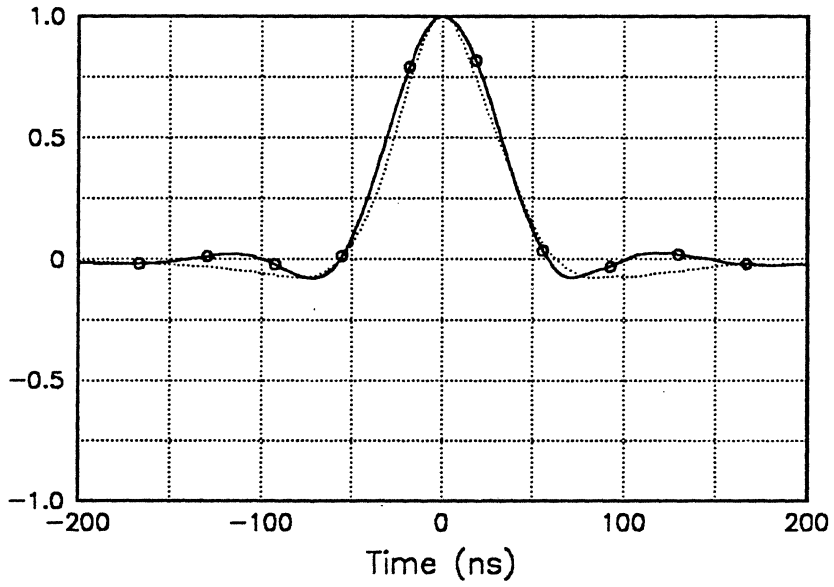

Figure 2. Isolated transition before (dotted) and after equalization for PRML at 3.0 MB/s.

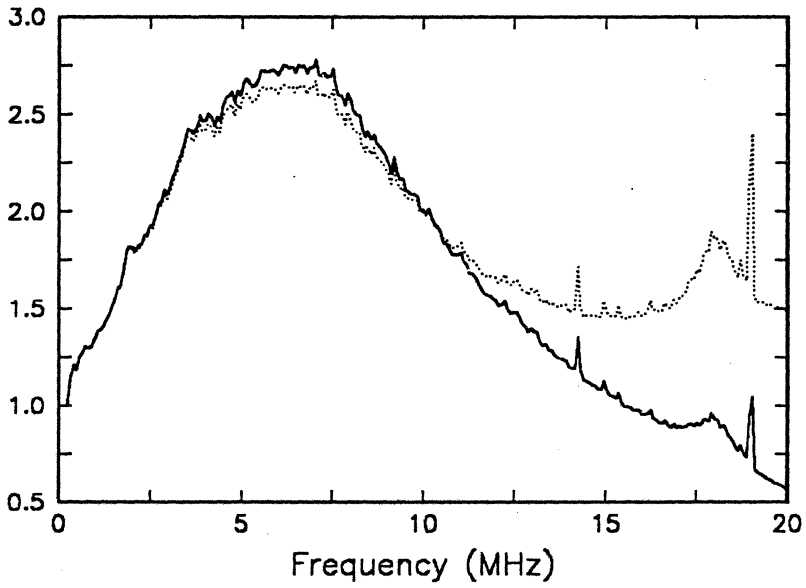

Figure 3. Noise spectrum before (dotted) and after equalization for peak detection at 3.0 MB/s.

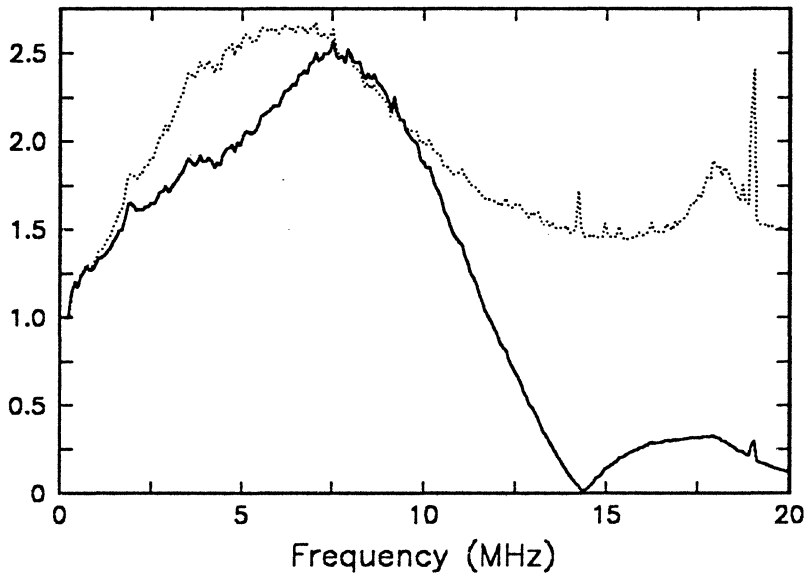

Figure 4. Noise spectrum before (dotted) and after equalization for PRML at 3.0 MB/s.

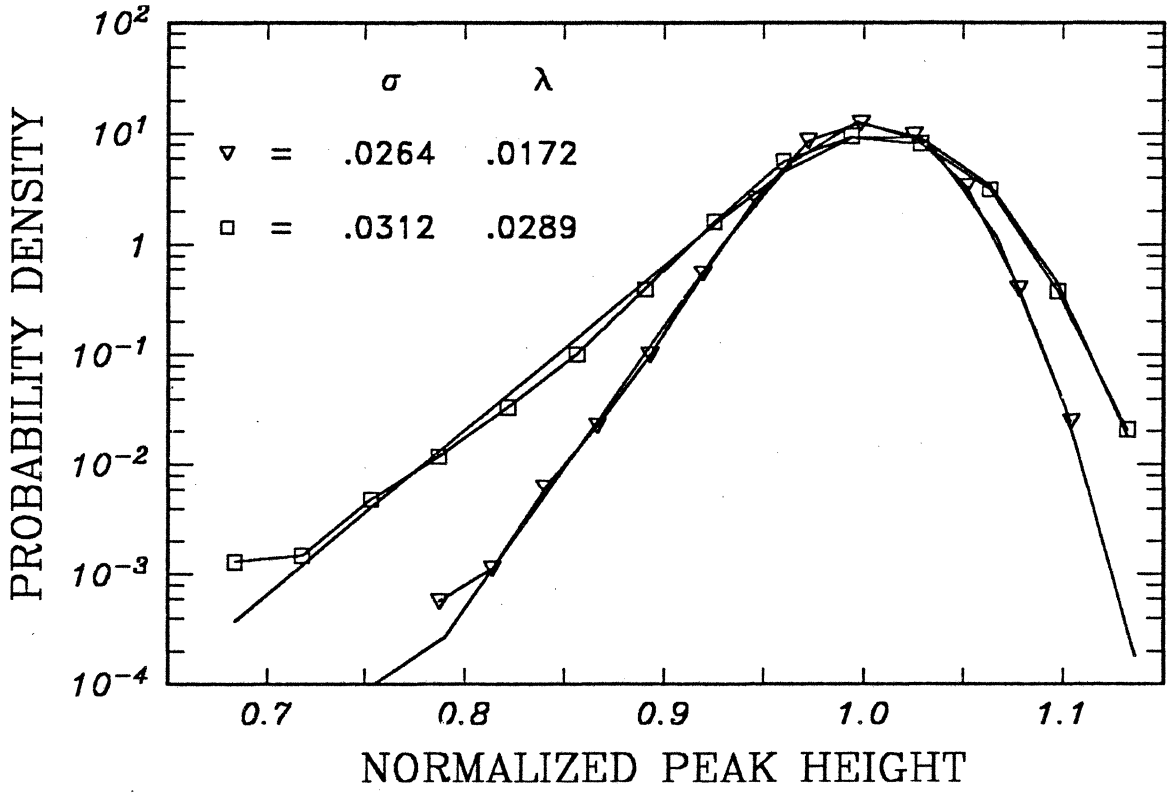

Figure 5. Peak amplitude distribution used for defect model

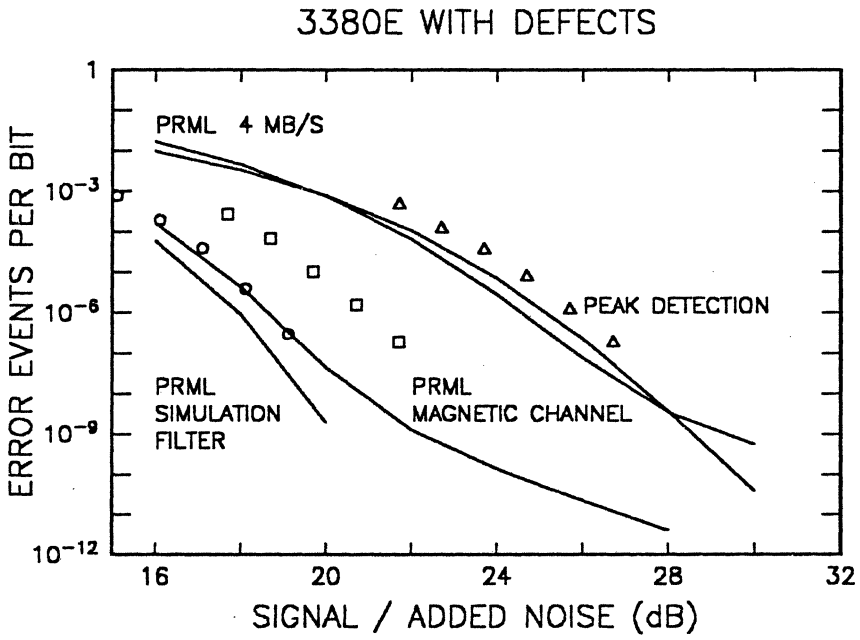

Figure 6. Error rate as a function of injected noise level. This graph shows modeled error rates at 3 MB/s for the 3380E (2,7)-coded peak detection channel, the PRML channel, and for an idealized PRML channel with no misequalization error. It includes a similar curve for the PRML channel at 4 MB/s. The measured results at 3 MB/s are included for comparison: △ = peak detection, □ = PRML/magnetic channel, ○ = PRML/channel simulation filter.

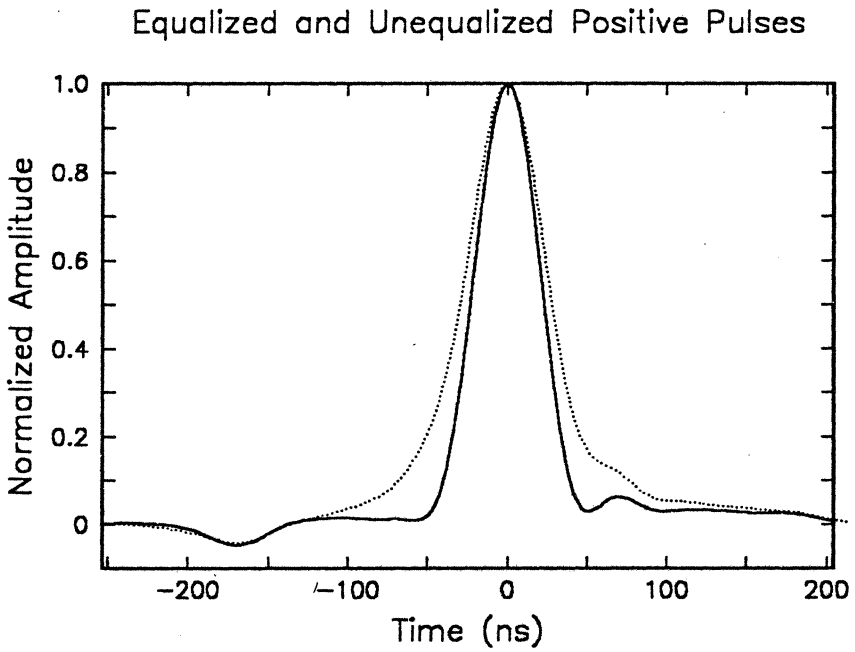

Figure 7. Isolated transition before (dotted) and after equalization for peak detection for MR head at 4.3 MB/s.

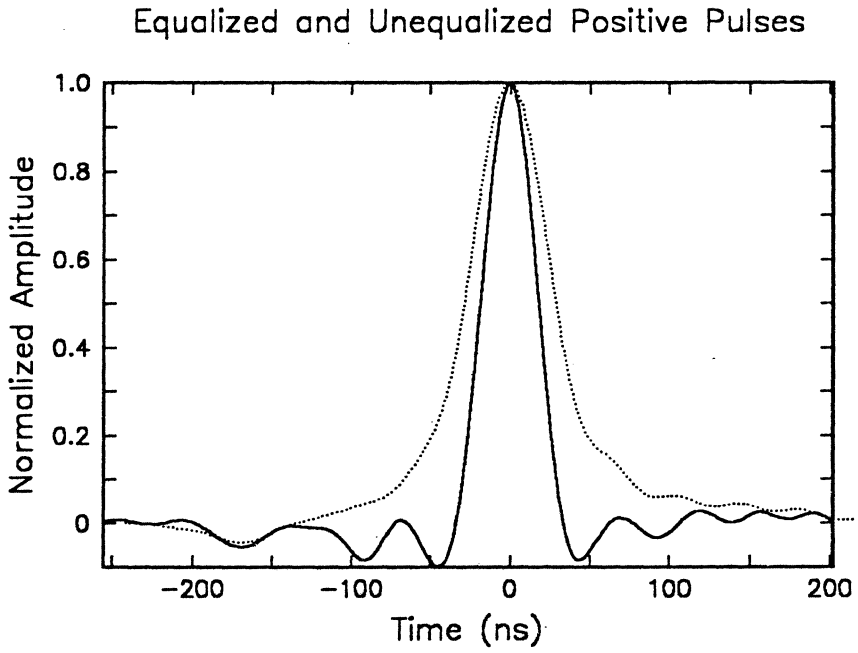

Figure 8. Isolated transition before (dotted) and after equalization for 17ML at 4.3 MB/s.

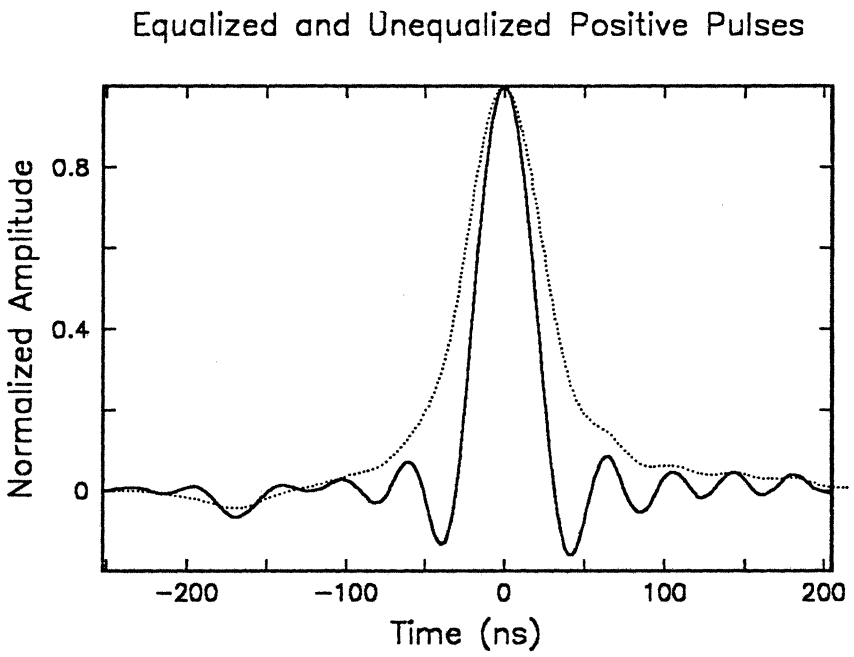

Figure 9. Isolated transition before (dotted) and after equalization for PRML at 4.3 MB/s.

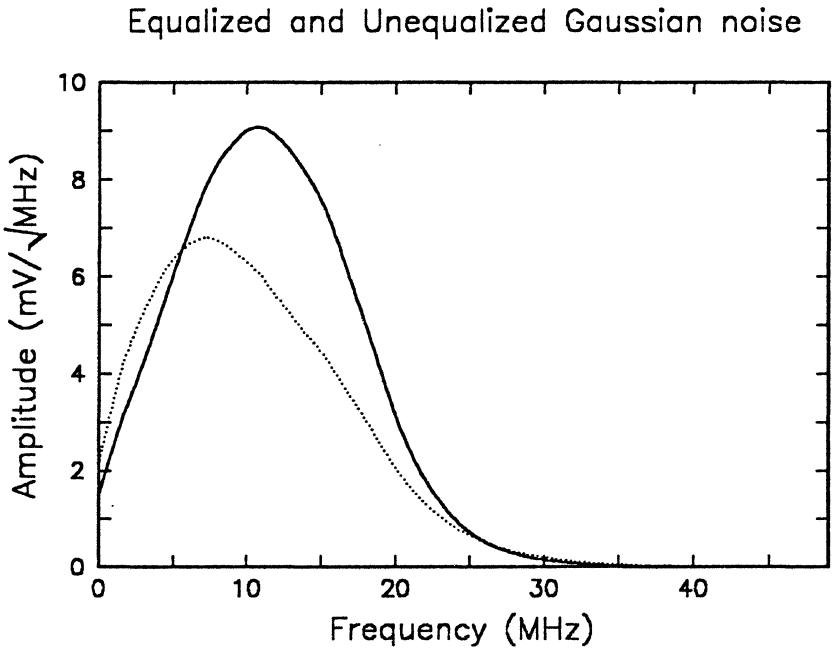

Figure 10. Noise spectrum before (dotted) and after equalization for peak detection at 4.3 MB/s.

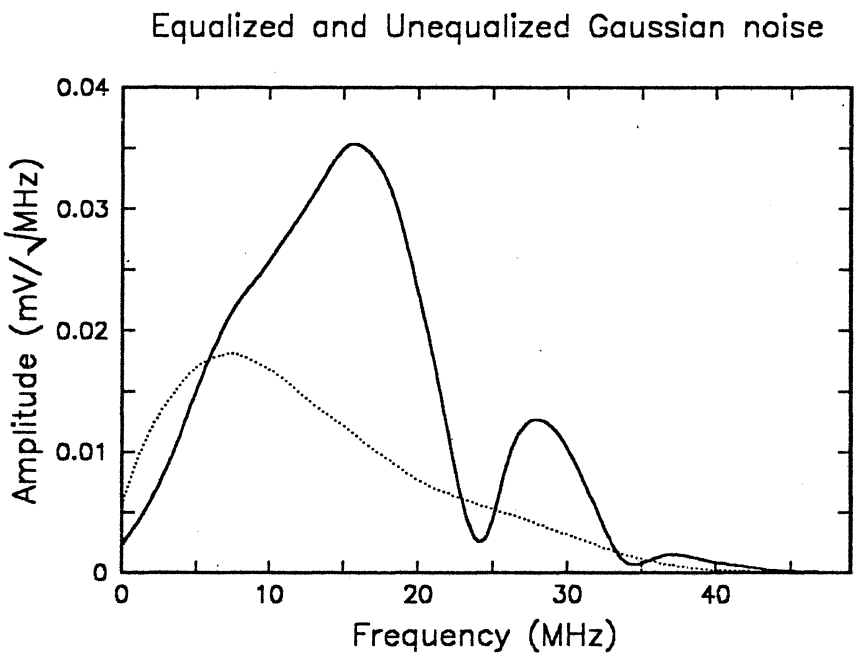

Figure 11. Noise spectrum before (dotted) and after equalization for 17ML at 4.3 MB/s.

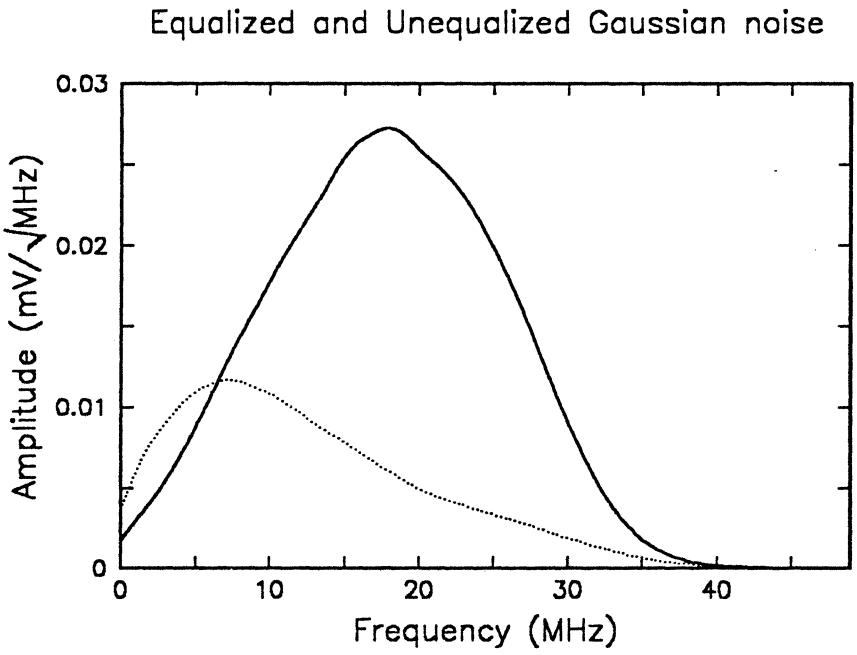

Figure 12. Noise spectrum before (dotted) and after equalization for PRML at 4.3 MB/s.

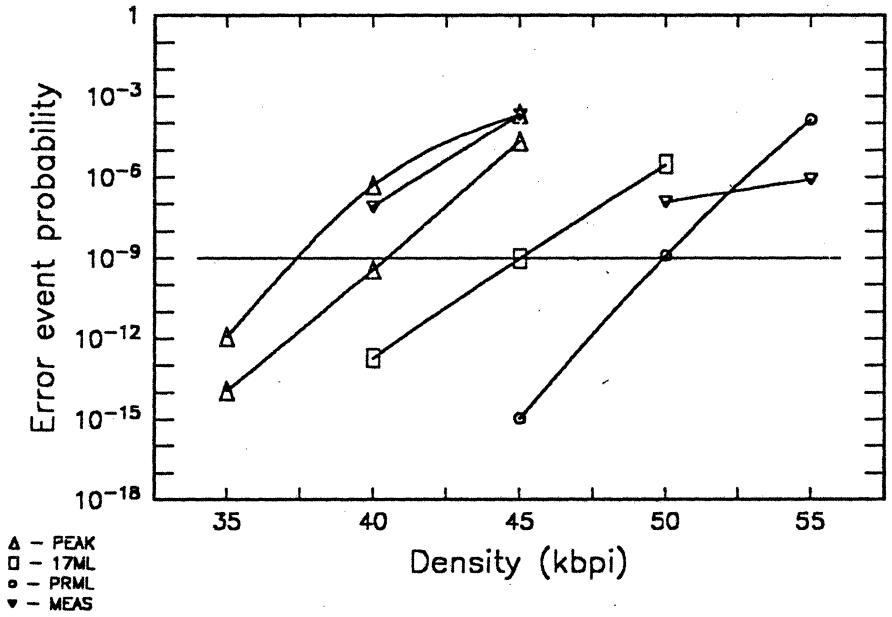

Figure 13. Error rate versus density under nominal conditions.

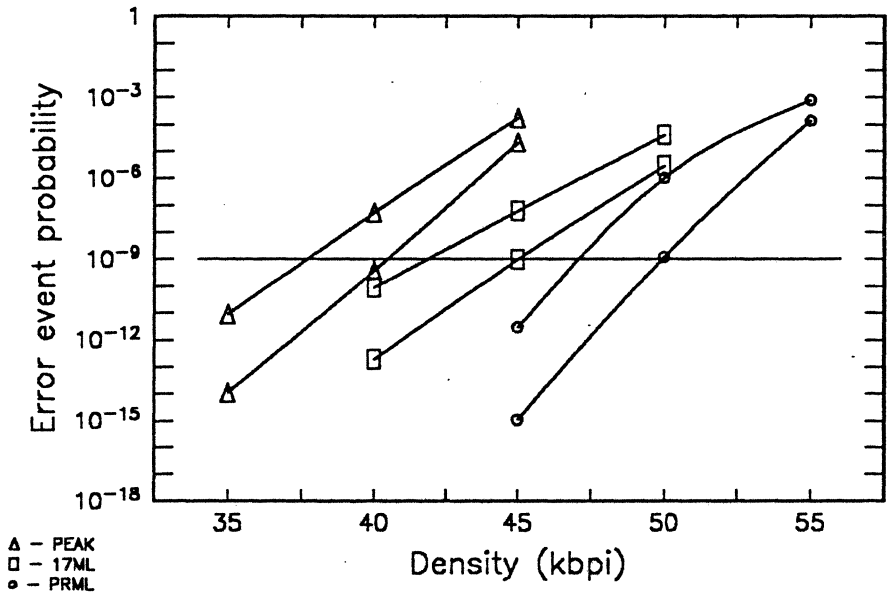

Figure 14. Error rate versus density with high noise.

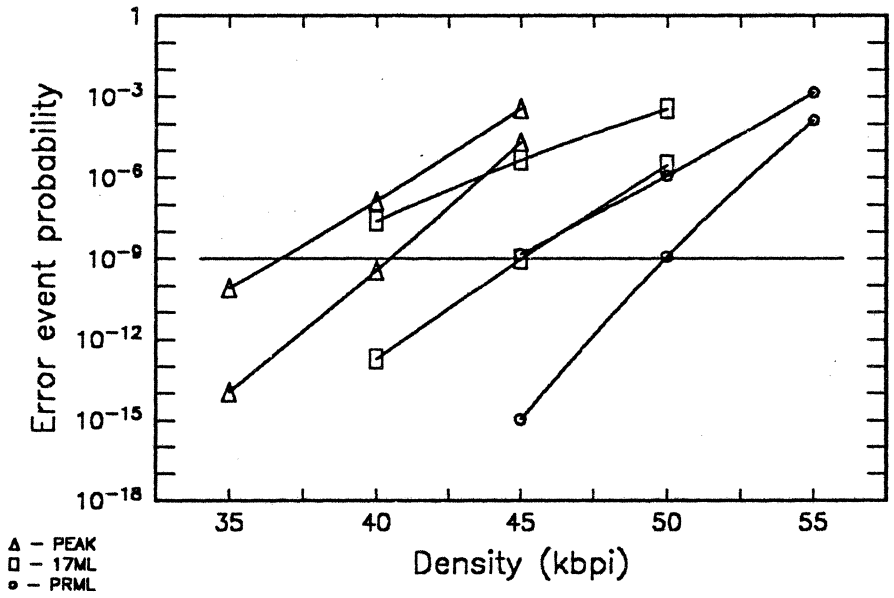

Figure 15. Error rate at a defect versus density.

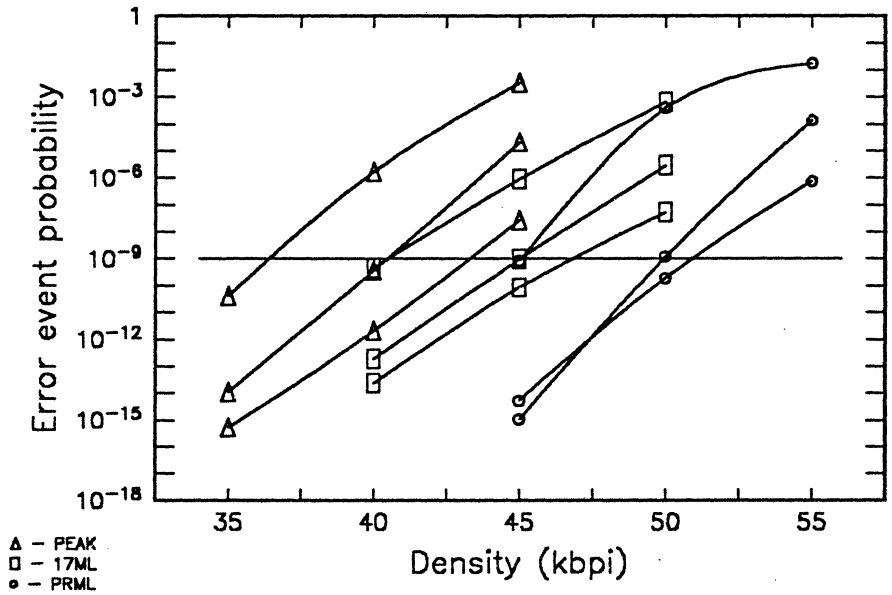

Figure 16. Error rate versus density with misequalization.

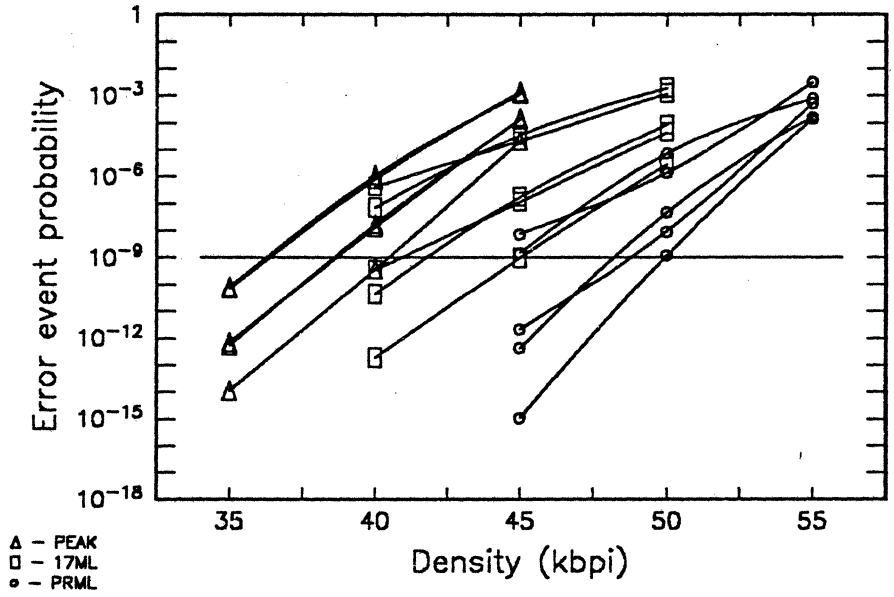

Figure 17. Error rate versus density with timing offsets.

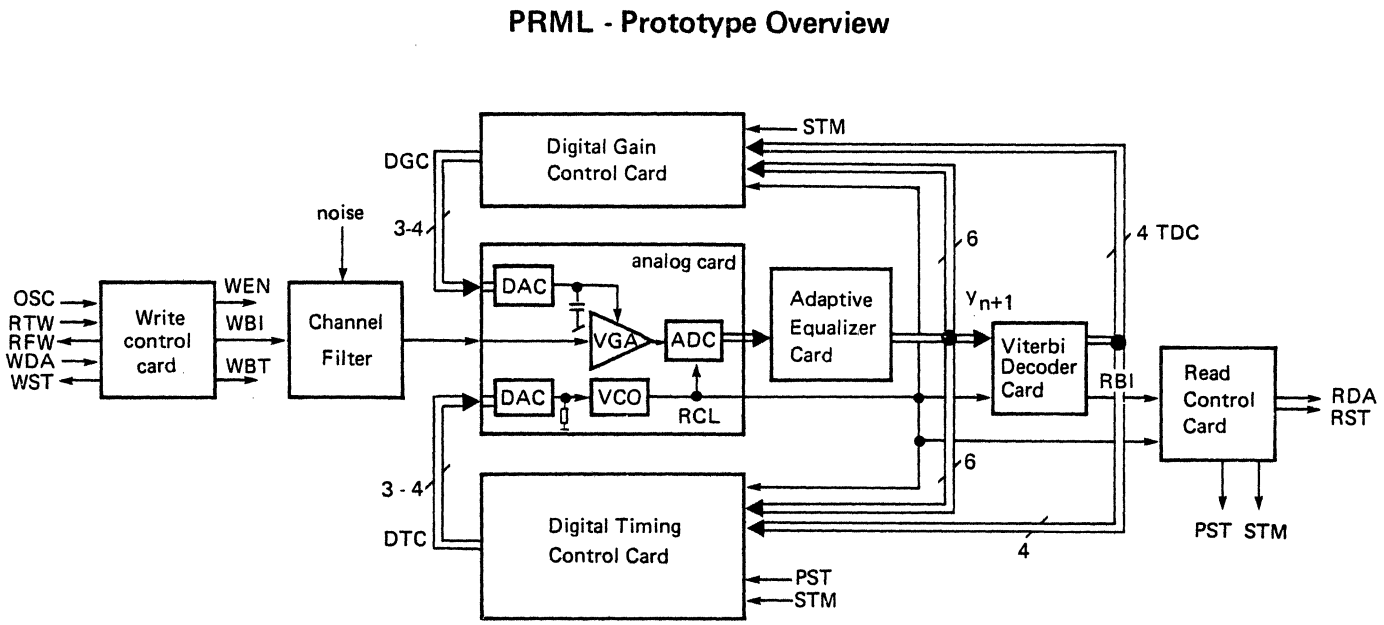

Figure 18. ZPRML Prototype system schematic.

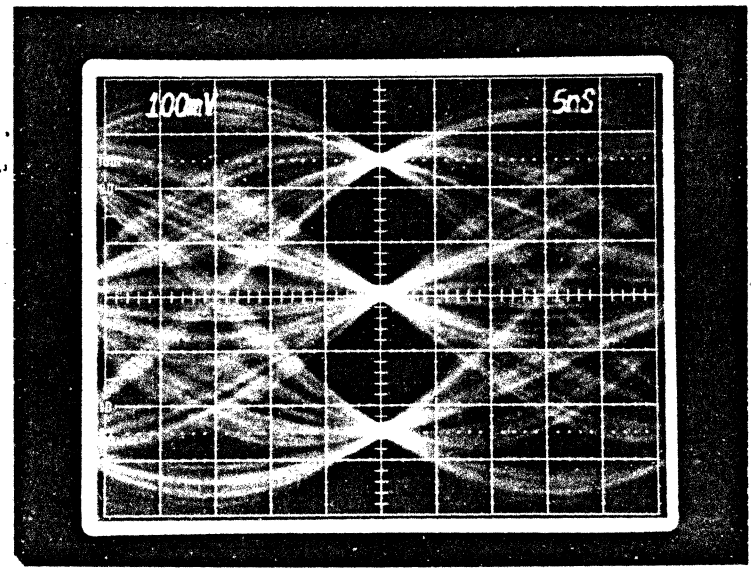

Figure 19. (a) Eye pattern for channel simulation filter at 3.0 MB/s

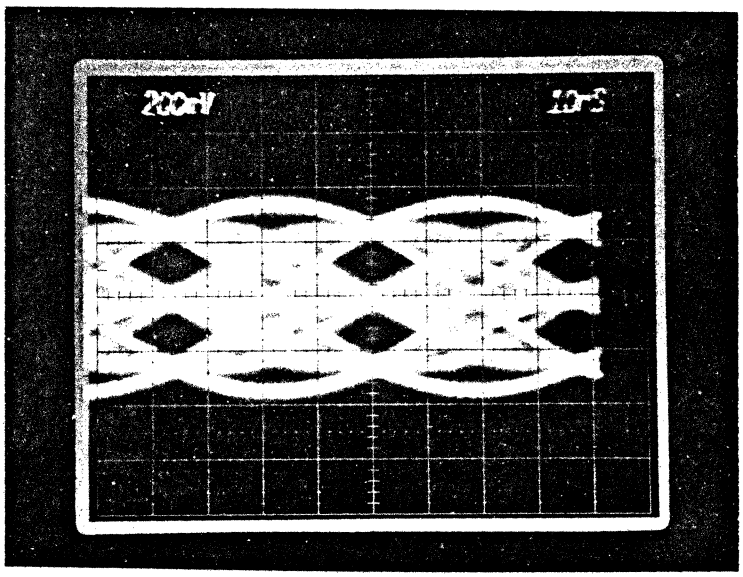

Figure 19. (b) Eye pattern for 3380E equalized signal at 3.0 MB/s

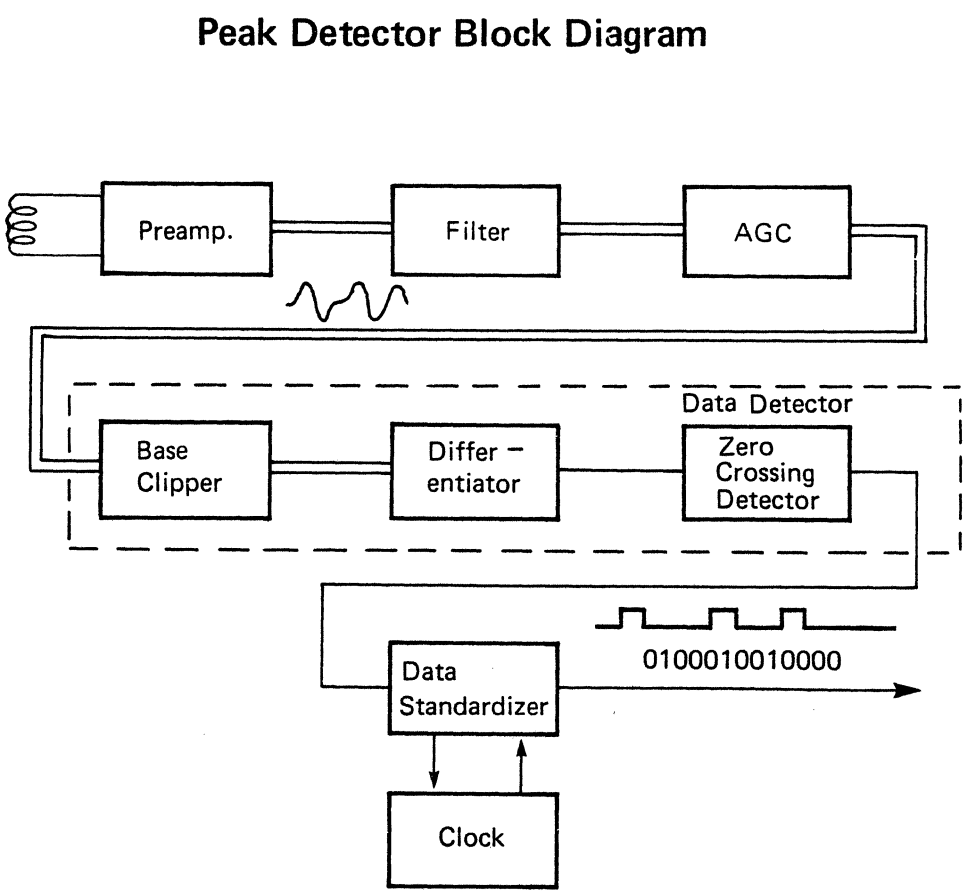

Figure 20. (2,7)-Coded Peak Detector System schematic.

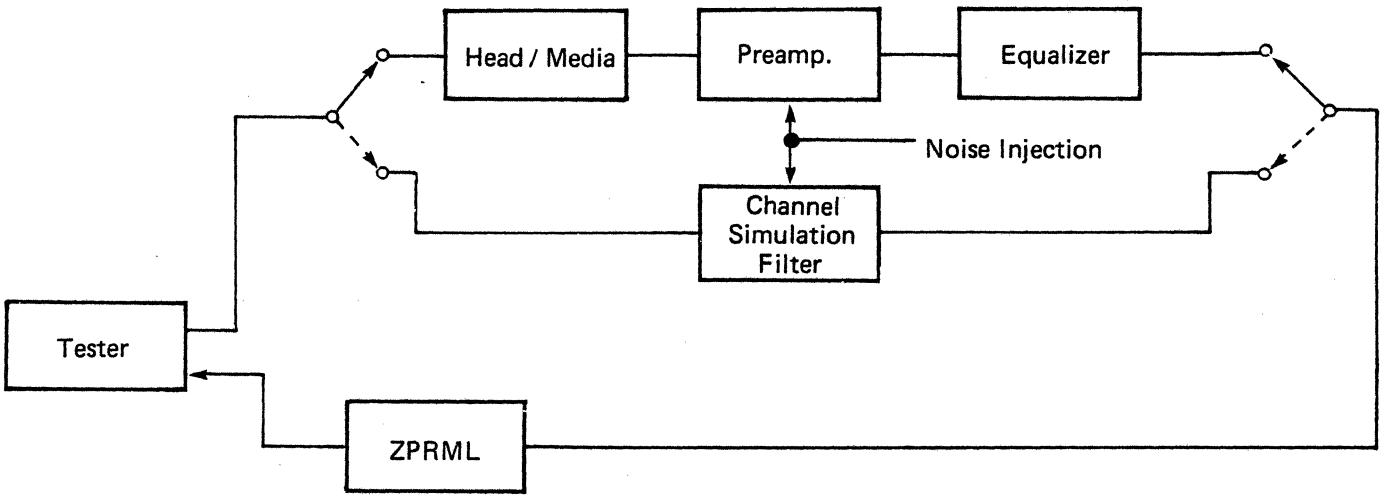

Figure 21. Experimental setup.

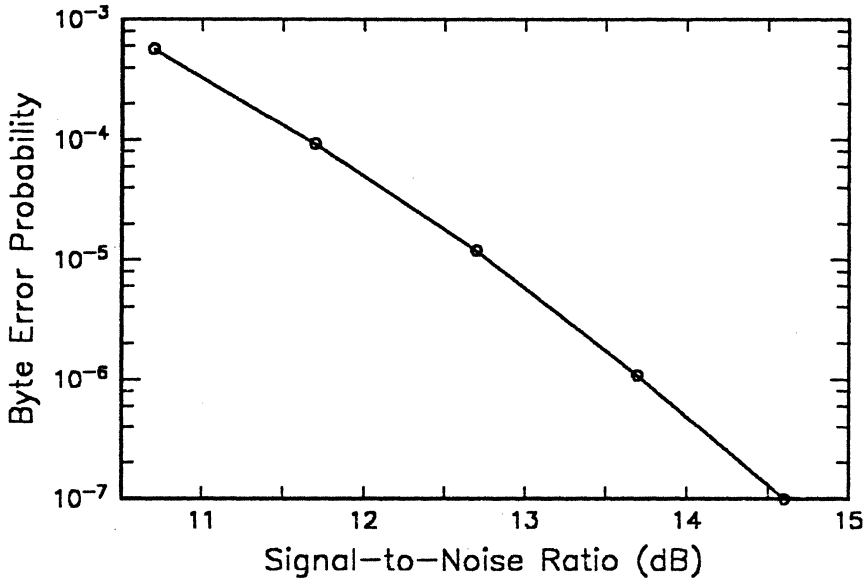

Figure 22. Byte error rate versus SNR for CSF at 3.0 MB/s.

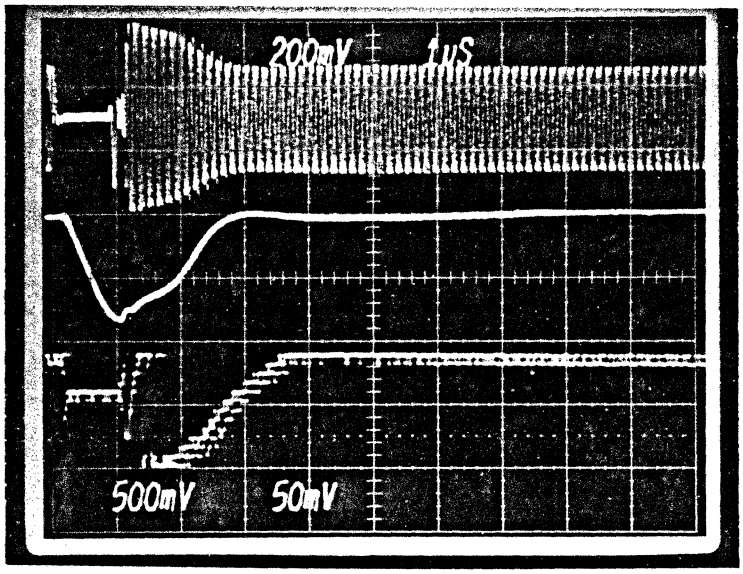

Figure 23. Transient Response of PRML control loops with 2% frequency offset. Input to ADC (top), VGA Control Voltage (middle), VFO control voltage (bottom).

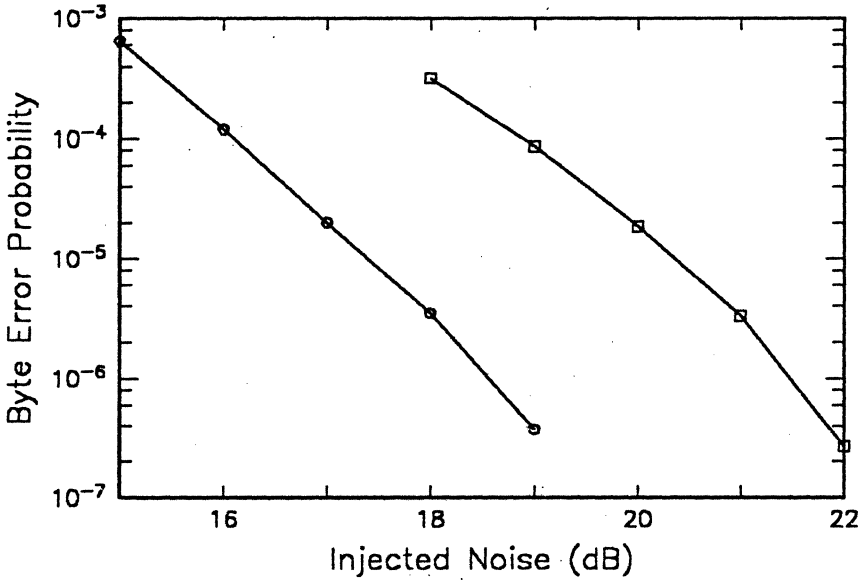

Figure 24. Error rate versus injected noise level at the OD at 3.0 MB/s. This plot is for the 3380E components: ○ = PRML, □ = (2,7)-coded peak detection.

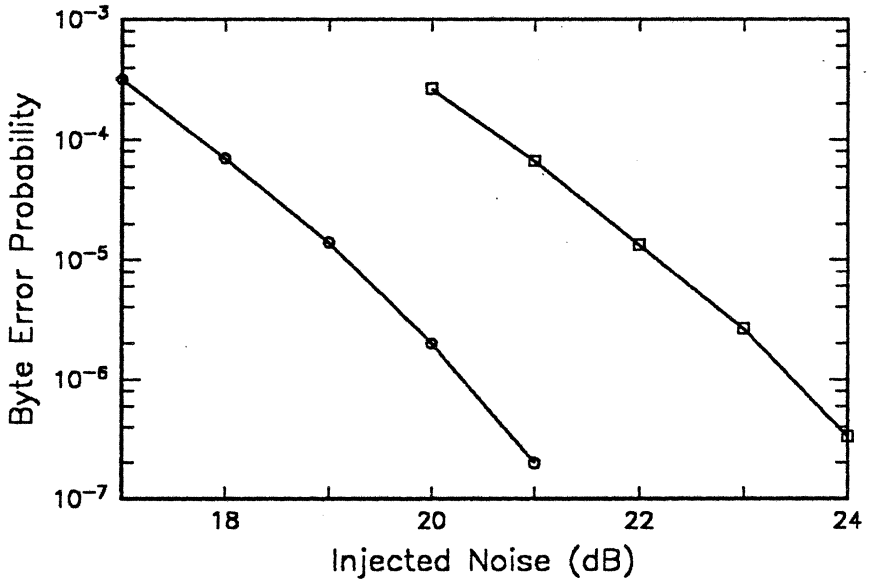

Figure 25. Error rate versus injected noise level at the MD at 3.0 MB/s. This plot is for the 3380E components: ○ = PRML, □ = (2,7)-coded peak detection.

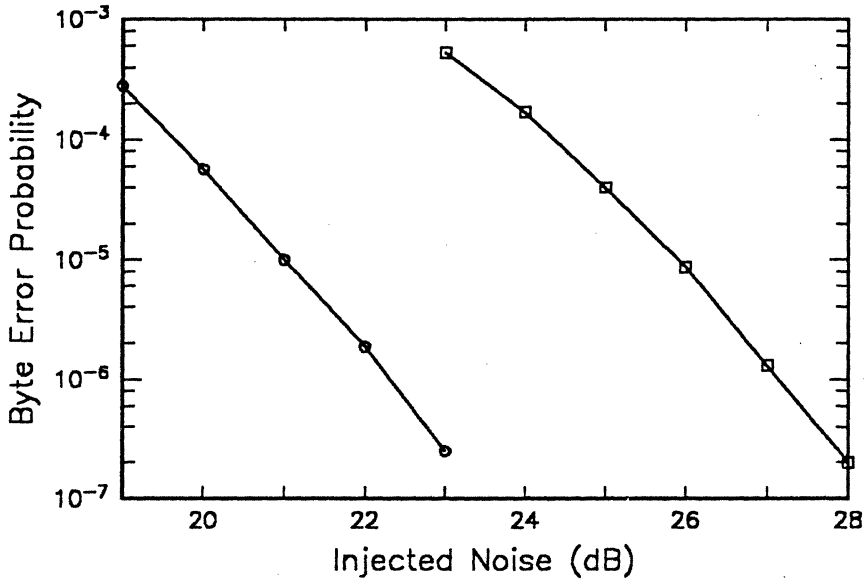

Figure 26. Error rate versus injected noise level at the ID at 3.0 MB/s. This plot is for the 3380E components: ○ = PRML, □ = (2,7)-coded peak detection.

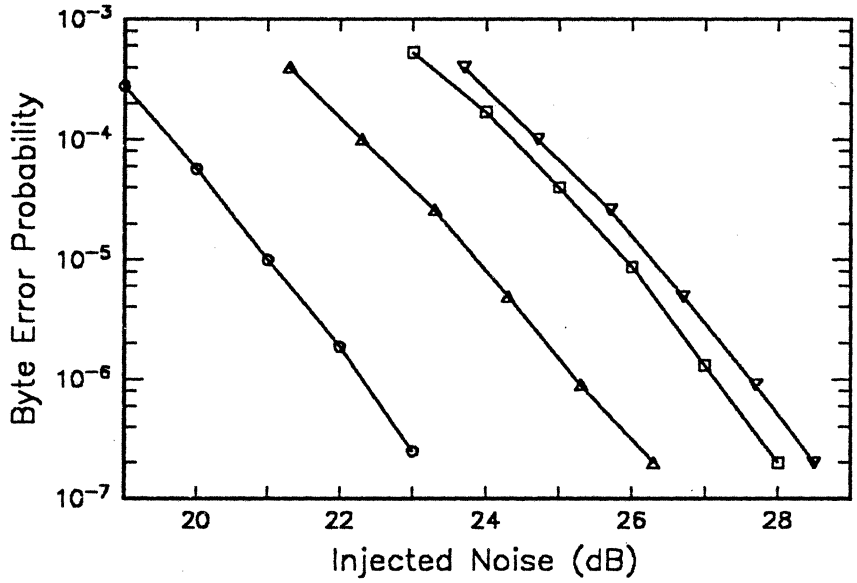

Figure 27. Error rate versus injected noise level at the ID. This plot compares the performance of (2,7) peak detection at 3.0 MB/s and PRML at 3.0, 3.6, and 3.9 MB/s on 3380E components: □ = (2,7) peak detection at 3.0 MB/s, ○ = PRML at 3.0 MB/s, △ = PRML at 3.6 MB/s, ∇ = PRML at 3.9 MB/s.

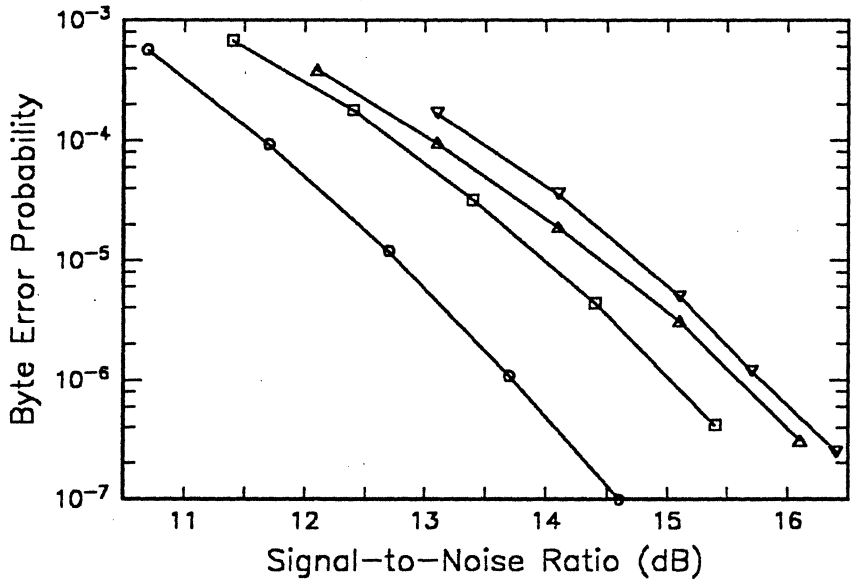

Figure 28. Error rate versus SNR for PRML on 3380E and ideal PRML. This plot compares the performance of PRML on 3380E components with that of ideal PRML on additive white Gaussian noise channel. All measurements are at 3.0 MB/s: ○ = ideal PRML, □ = PRML on 3380E (OD), △ = PRML on 3380E (MD), ∇ = PRML on 3380E (ID).

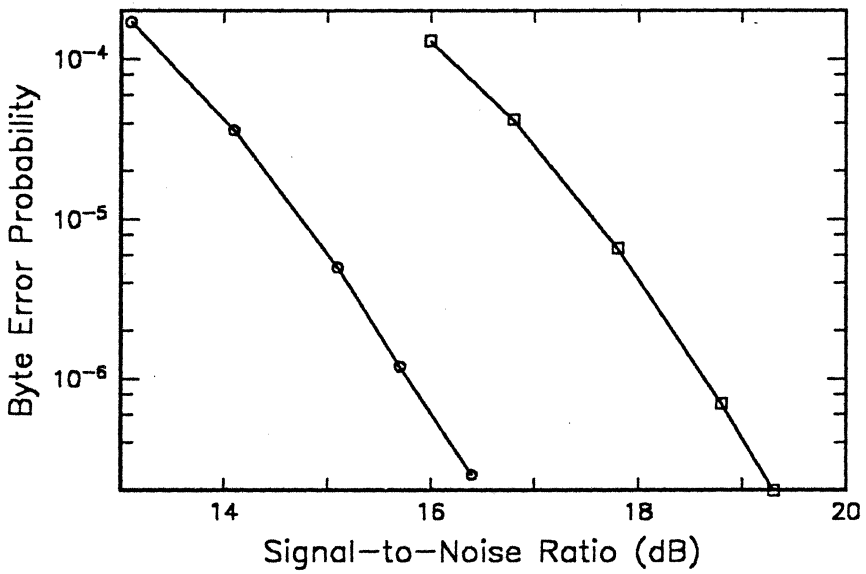

Figure 29. (a) Performance of PR4 with final and first tentative decisions. This plot compares the performance of maximum-likelihood and first tentative decisions on 3380E components at the OD: ○ = PR4 with final decisions, □ = PR4 with first tentative decisions.

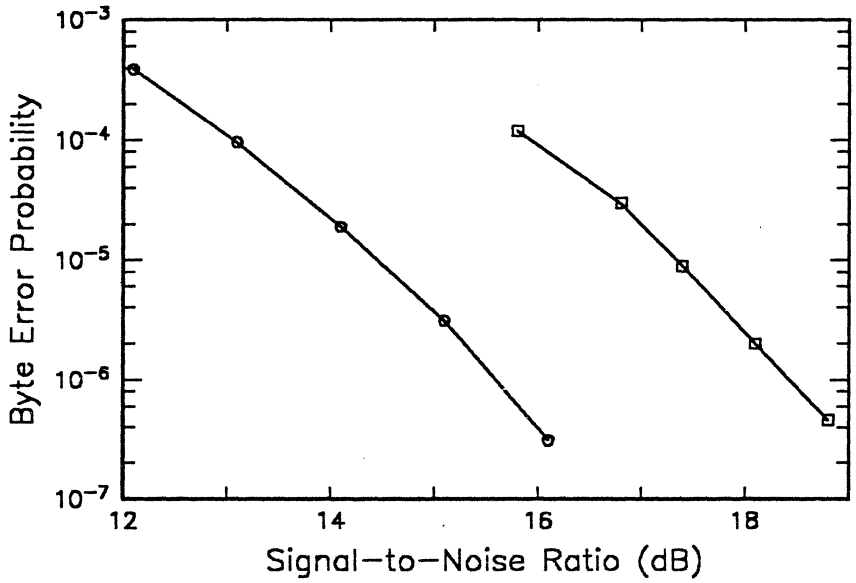

Figure 29. (b) Performance of PR4 with final and first tentative decisions. This plot compares the performance of maximum-likelihood and first tentative decisions on 3380E components at the MD: ○ = PR4 with final decisions, □ = PR4 with first tentative decisions.

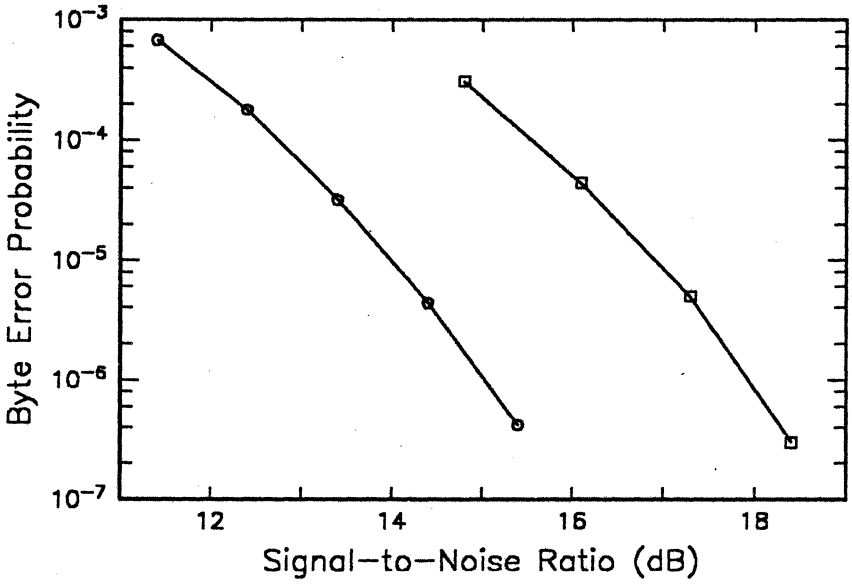

Figure 29. (c) Performance of PR4 with final and first tentative decisions. This plot compares the performance of maximum-likelihood and first tentative decisions on 3380E components at the ID: ○ = PR4 with final decisions, □ = PR4 with first tentative decisions.

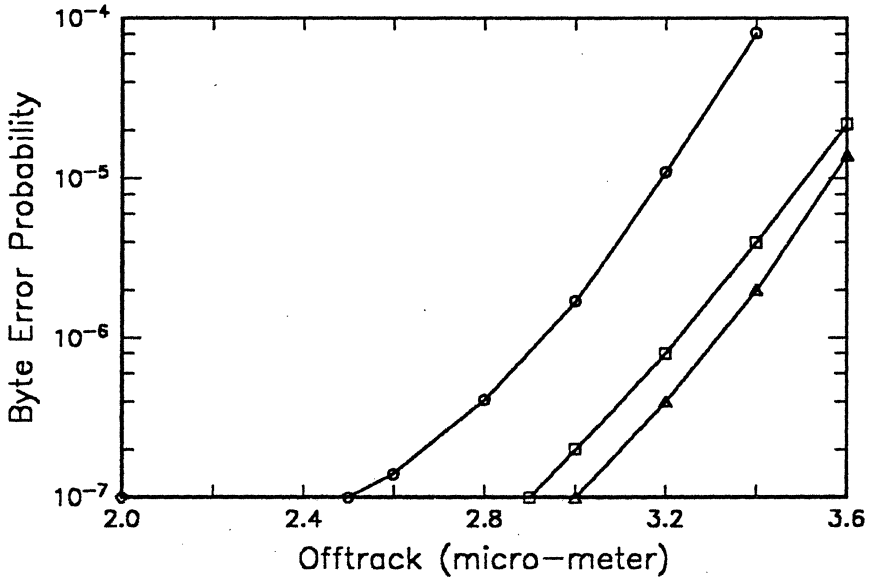

Figure 30. Off-track performance comparison at 3.0 MB/s. This plot compares the offtrack performance of PRML and (2,7) peak detection on 3380E components: ○ = (2,7) peak detection at the ID, △ = (2,7) peak detection at the MD and OD, □ = PRML at the OD, MD, and ID.

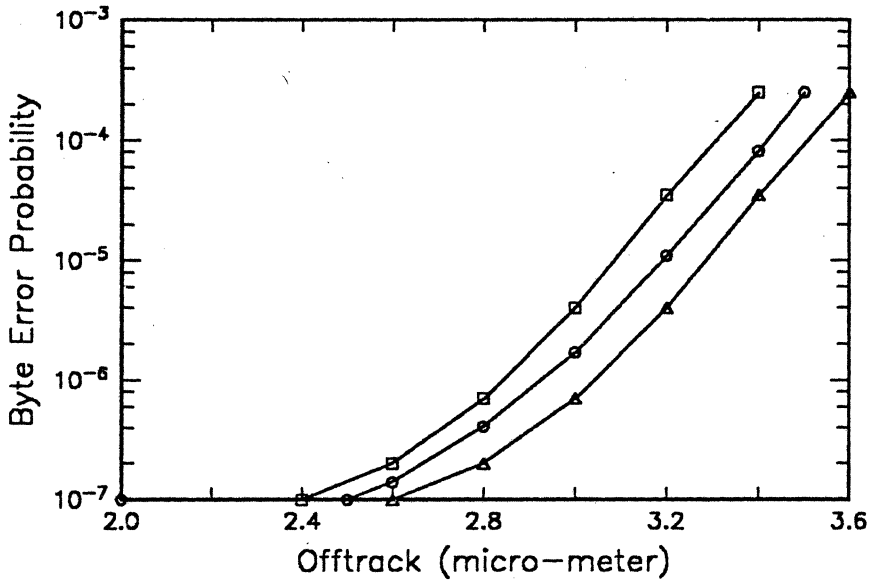

Figure 31. Off-track performance of 3.0 MB/s peak detection and 3.9 MB/s PRML. This plot compares the performance of (2,7) peak detection at 3.0 MB/s and PRML at 3.9 MB/s on 3380E components at the ID and also shows the effect of synchronization pattern on the performance of PRML: ○ = (2,7) peak detection at 3.0 MB/s, △ = PRML at 3.9 MB/s with random data interference, □ = PRML at 3.9 MB/s with synchronization pattern interference.

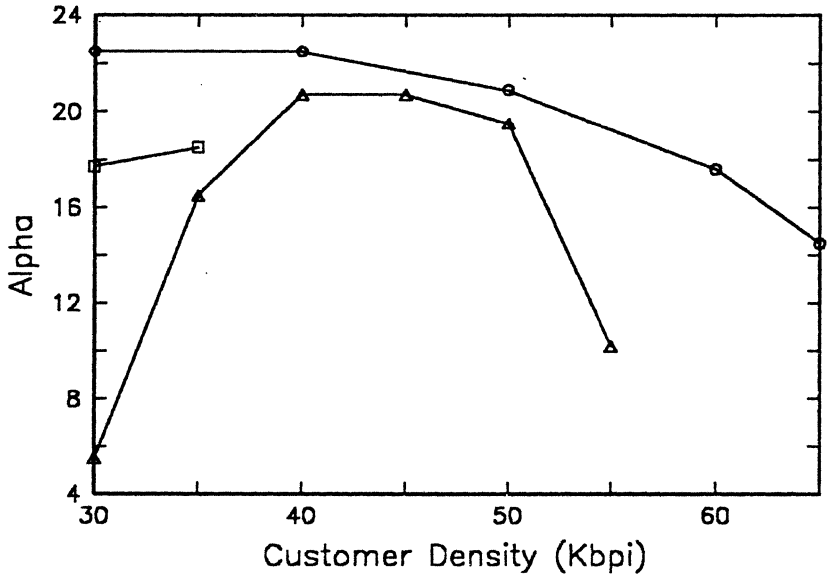

Figure 32. (a) Performance of PRML and (1,7) peak detection on MR head/particulate disk. This plot compares alpha versus linear density for PRML and (1,7) peak detection with a 8.75 μm MR head: ○ = PRML, □ = (1,7) peak detection without equalization, △ = (1,7) peak detection with equalization.

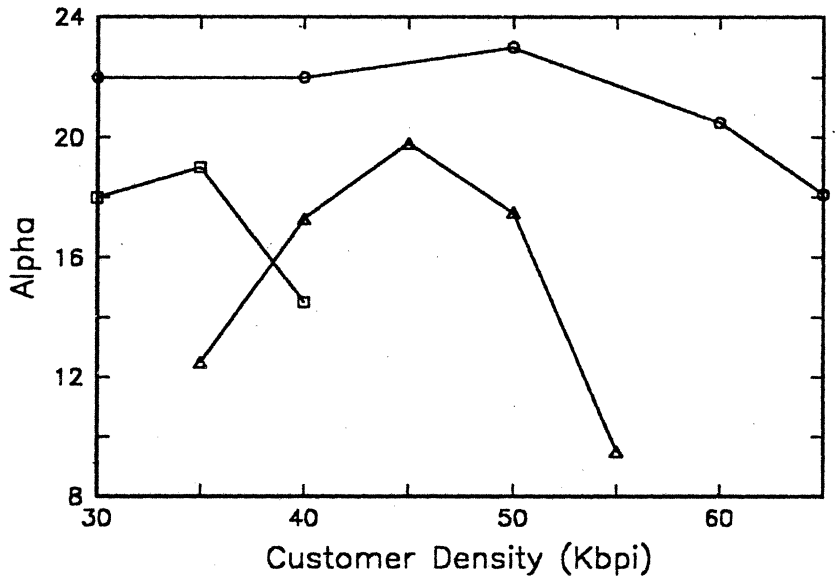

Figure 32. (b) Performance of PRML and (1,7) peak detection on MR head/particulate disk. This plot compares alpha versus linear density for PRML and (1,7) peak detection with a 6.75 μm MR head: ○ = PRML, □ = (1,7) peak detection without equalization, △ = (1,7) peak detection with equalization.

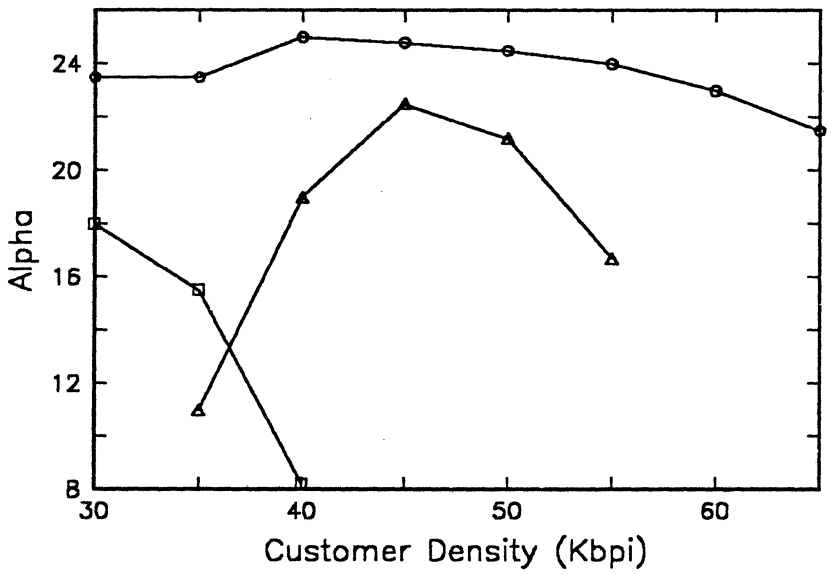

Figure 32. (c) Performance of PRML and (1,7) peak detection on MR head/particulate disk. This plot compares alpha versus linear density for PRML and (1,7) peak detection with a 6.00 μm MR head: ○ = PRML, □ = (1,7) peak detection without equalization, △ = (1,7) peak detection with equalization.

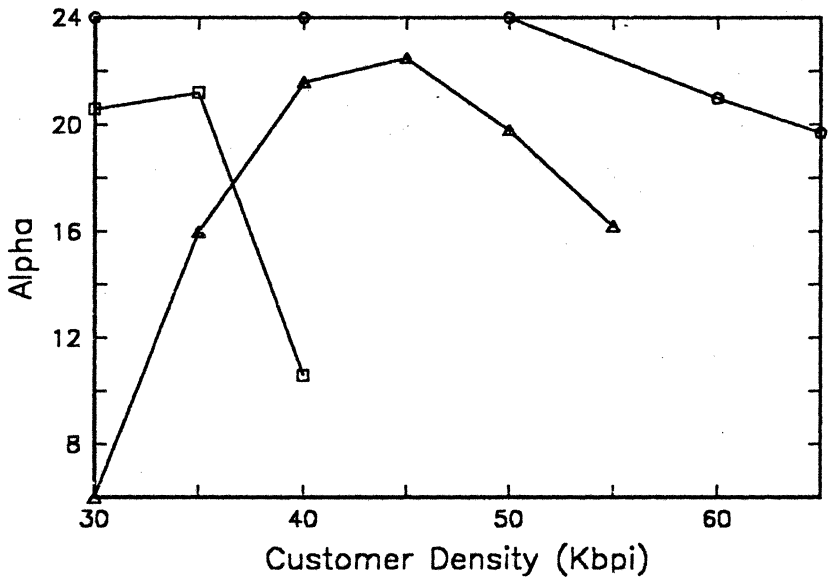

Figure 32. (d) Performance of PRML and (1,7) peak detection on MR head/particulate disk. This plot compares alpha versus linear density for PRML and (1,7) peak detection with a 5.25 μm MR head: ○ = PRML, □ = (1,7) peak detection without equalization, △ = (1,7) peak detection with equalization.

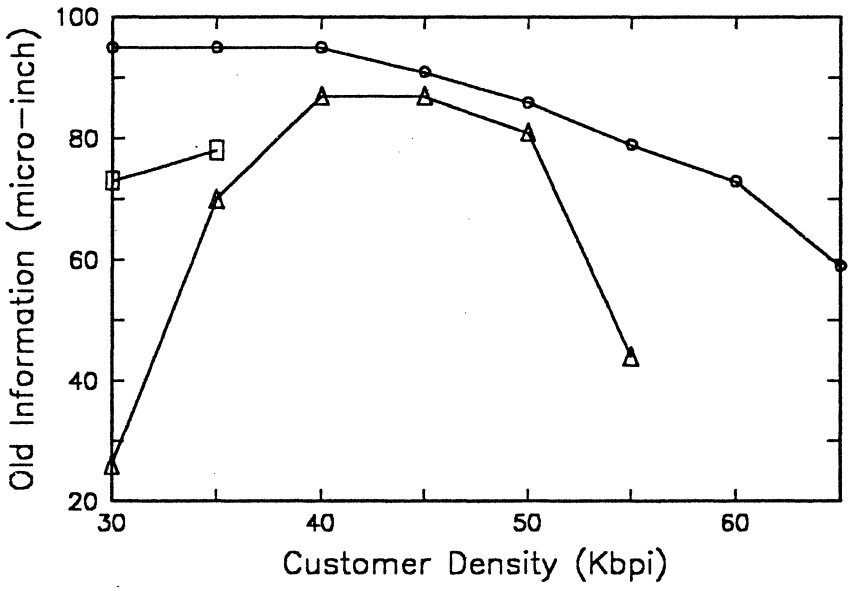

Figure 33. (a) Performance of PRML and (1,7) peak detection on MR head particulate disk. This plot compares old information number versus linear density of PRML and (1,7) peak detection using a 8.75 μm MR head: ○ = PRML, □ = (1,7) peak detection without equalization, △ = (1,7) peak detection with equalization.

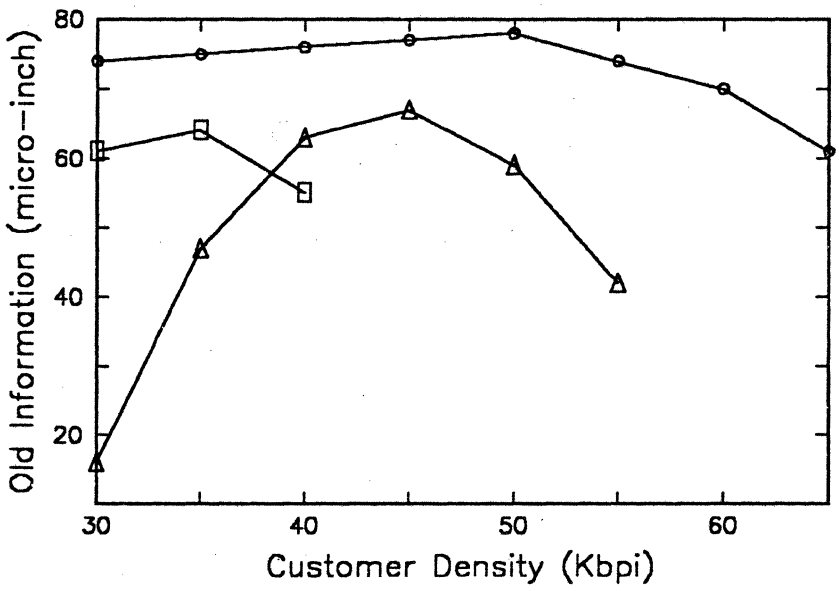

Figure 33. (b) Performance of PRML and (1,7) peak detection on MR head/particulate disk. This plot compares old information number versus linear density of PRML and (1,7) peak detection using a 6.75 μm MR head: ○ = PRML, □ = (1,7) peak detection without equalization, △ = (1,7) peak detection with equalization.

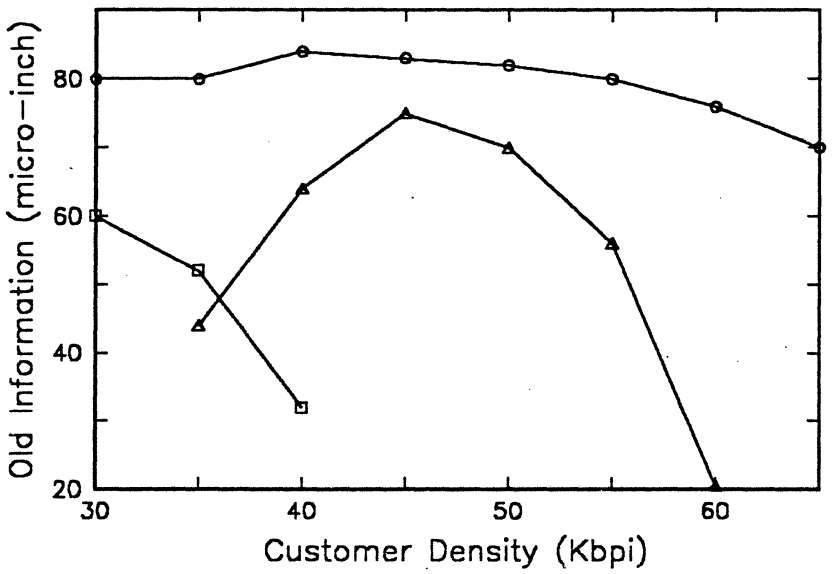

Figure 33. (c) Performance of PRML and (1,7) peak detection on MR head/particulate disk. This plot compares old information number versus linear density of PRML and (1,7) peak detection using a 6.00 μm MR head: ○ = PRML, □ = (1,7) peak detection without equalization, △ = (1,7) peak detection with equalization.

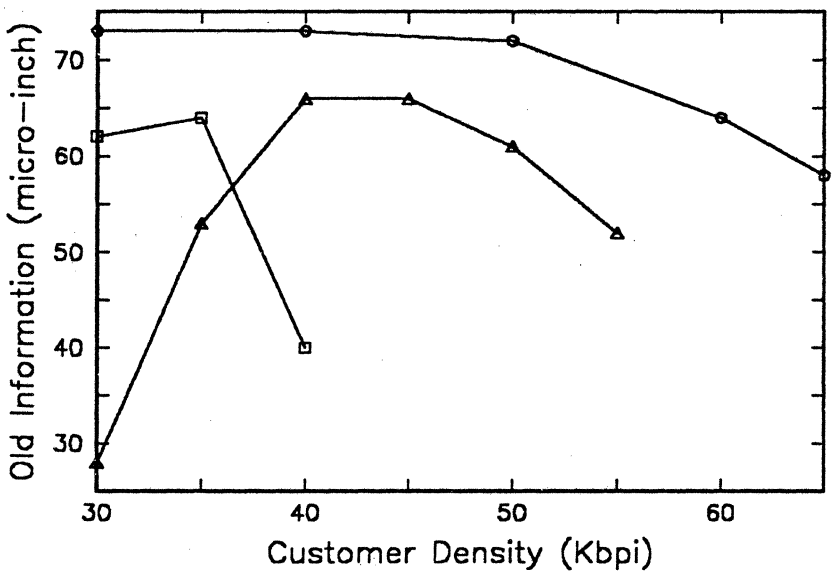

Figure 33. (d) Performance of PRML and (1,7) peak detection on MR head/particulate disk. This plot compares old information number versus linear density of PRML and (1,7) peak detection using a 5.25 μm MR head: ○ = PRML, □ = (1,7) peak detection without equalization, △ = (1,7) peak detection with equalization.

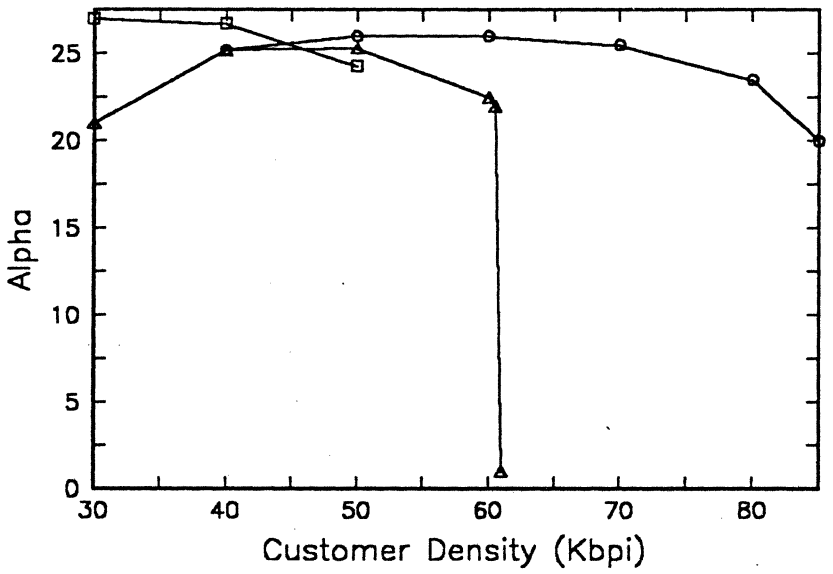

Figure 34. Alpha versus linear density on MR head/film disk. ○ = PRML, □ = (1,7) peak detection without equalization, △ = (1,7) peak detection with equalization.

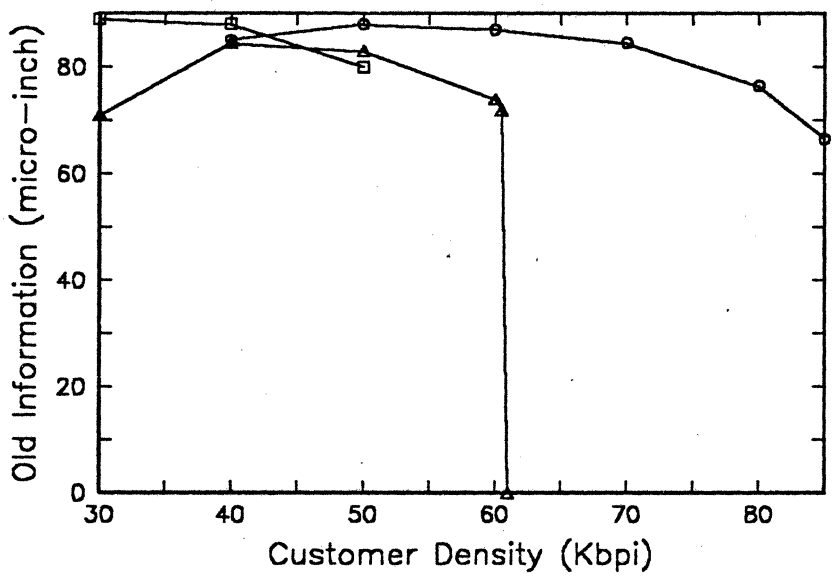

Figure 35. Old information versus linear density on MR head/film disk. ○ = PRML, □ = (1,7) peak detection without equalization, △ = (1,7) peak detection with equalization.